Master's thesis

2022

Abhishek Mahajan

NTNU
Norwegian University of
Science and Technology
Faculty of Medicine and Health Sciences
Kavli Institute for Systems Neuroscience

Abhishek Mahajan

Evidence for ecological resonance

December 2022

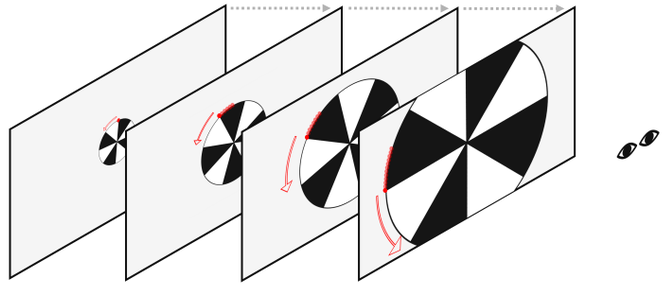

NTNU
Norwegian University of
Science and Technology

NTNU
Norwegian University of
Science and Technology

NTNU
Norwegian University of
Science and Technology

Evidence for ecological resonance

Abhishek Mahajan

MSc Neuroscience
Submission date: December 2022
Supervisor: Audrey van der Meer
Co-supervisor: NA

Norwegian University of Science and Technology
Kavli Institute for Systems Neuroscience

Abstract

In the ecological psychology approach, an organism and the environment encapsulating the organism are studied as a single dynamical system, with different scales of operation. Evidence based on neural underpinnings to showcase the inner workings of these different scales is scarce. Ecological resonance is claimed to occur between the ecological scale and the neural scale, where some variable X in neural dynamics N_D is purported to be coupled with perceptual information Ψ.

The purpose of the current study was to find evidence for ecological resonance. A new visual motion perception study was designed to work with high density electroencephalography (HD EEG) for this purpose. 12 adults were recruited to look at a visual stimulus that combined looming and rotational motion dynamics. At the neural scale, time-frequency domain analysis was prioritised to search for neural dynamics, guided by the frequency related optical dynamics in the stimulus at the ecological scale.

A linear relationship was found between the frequency components from fast Fourier transform (FFT) of a 32.5Hz band in time spectral evolution (TSE) vs. the frequency of return to orientation. The coupling parameter k was found to be 2.468 and 8.226, with the sum of squares due to error (SSE) equal to 0.03206 and 0.1283 for participants O (in VCrL) and T (in VClR) respectively.

The low SSE values suggest a linear coupling relationship between the perceptual information particular to this study, and the frequency components derived from the FFT of 32.5Hz TSE band, representing neural dynamics. This suggests strong preliminary evidence in favour of ecological resonance. We suspect a cycling between multiple neuronal assemblies to respond to the ongoing stimuli, as a plausible biological explanation for the meaning behind FFT measure and a reason of sustained ERD.

Acknowledgments

I would like to thank Dr Audrey van der Meer for her guidance and for giving me the opportunity to do my thesis at NuLab, NTNU.

Yogesh, Seth, Vegard, Kenneth, Sukanya, Ivan, Stian, Rohit, Prabhav, Silje N have always been gracious to discuss when I needed and generous to share their knowledge with me.

Hans, Tom, Silje, Vegard thank you, for your help with data and hardware related issues.

I am deeply grateful to all the participants, who were kind enough to take out their time for science!

Lastly, my parents deserve the most credit for helping me navigate this challenging pursuit.

Table of Contents

List of Figures

List of Tables

List of Equations

List of Abbreviations (or Symbols)

DPI	Dots per inches
NTNU	The Norwegian University of Science and Technology
PDF	Portable Document Format
cm	centimetres
EGI	Electrical Geodesic, Inc
GSN	Geodesic Sensor Net
MS	Microsoft
HD EEG	High Density Electroencephalography
KCl	Potassium Chloride (electrolytic salt)
PC	Personal Computer (Desktop)
.mff	Metafile format
A.C.	Alternating current
PCA	Principal Component Analysis
TSE	Time Spectral Evolution
SD	Standard Deviation
Hz,ms	Hertz, milliseconds
VEP	Visual Evoked Potentials
BESA	Brain Electrical Source Analysis software
TFA	Time-frequency analysis
TSE	Time spectral evolution
ERD/ERS	Event related desynchronization/synchronization
FFT	Fast fourier transform

1 Introduction

J.J. Gibson (1966, 1979) first came up with ecological psychology. A fundamental feature of ecological psychology as opposed to cognitive psychology is that it is based on direct realism. It also assumes and vehemently argues in favour of the richness of stimulus, as opposed to the cognitivist idea where poverty of stimulus is assumed (Chomsky, 1980).

Gibson came up with the term 'affordance' the ability of an organism to detect useful information in the environment surrounding it, to perceive any opportunity of action.

Ecological Psychology considers the organism and the environment inside which the organism perceives, as a single dynamical system. The environment and organism's interaction together fuels perception. This can be understood with a basic concept like optic flow in the everyday world. Humans by design can distinguish and comprehend the world around them while moving, as well as while static. It's this moving what we are interested in.

So far tau-coupling analyses has been used to show the working mechanism, that show coupling at the ecological, behavioural and the neural scales. Tau coupling analyses is based on the General tau theory by D.N. Lee (2009), where the tau measures the action gap. Tau can be calculated for multiple quantities. In fact, a study by van der Weel and van der Meer (2009) uses tau of loom with respect to the tau of source waveform to show tau coupling between the ecological scale and the neural scale for infants.

Resonance is a general concept. To put it simply, when two bodies interact, and one drives the other with external force, the driven body is said to resonate with the driving body.

Raja, V (2018) considers the previous example as a biological plausibility for the concept of ecological resonance. Raja quotes Gibson

> "Instead of supposing that the brain constructs or computes the objective information from a kaleidoscopic inflow of sensations, we may suppose the orienting of the organs of perception is governed by the brain so that the whole system of input and output resonates to the external information."

to pick apart the term resonance, and coin ecological resonance. He explains ecological resonance as the phenomena that goes on inside an organism (in CNS), with respect to what goes on at the ecological scale.

To specify it further and formulate it formally, he comes up with a relationship:

$$O\text{-}E_D = G(\psi,t) \ldots (i)$$

$$N_D = F(\chi,t), \text{ where } \chi = k\psi \ldots (ii)$$

Here the $O\text{-}E_D$ represents environment-agent dynamics, modulated by Ψ in time (t). N_D represents the neural dynamics, function of some variable χ in time (t). Ψ is the perceptual information present in the environment-agent dynamics. An example of this is 'tau' by Lee (2009). Tau is a ratio-based measure that measures gap closure. 'k' is the coupling parameter, which suggests a coupling between the ecological and the neural scale.

1.1 Research Objectives

a) Design an experiment using the looming paradigm that contains measurable frequency parameter
b) Look at time-frequency analysis to determine the response to the stimulus and hunt for relationships between the stimuli parameter and the time-frequency response
c) Model input (ecological scale) output (neural scale) relationship

1.2 Hypothesis

Research question is, if one can find a direct link in the spatial frequency of stimulus and time-frequency domain components of the EEG signal?

Hypothesis: If ecological resonance is plausible, there must exist an ecological variable (or perceptual information) that satisfies the conditions:

a) variation in neural activity is strongly correlated to the variation in the ecological variable. (Biological plausibility)
b) neural dynamics contain an ecological variable as one of the parameters.

2 Methodology

To find the evidence for ecological resonance, we decided to pursue visual motion perception and record brain signals with HD EEG. This section expounds the experimental design and analysis techniques.

2.1 Experiment

An overview of the experimental setup is provided, followed by detailed experimental design steps. At the end, the perceptual information measured at the ecological scale is explained.

2.1.1 Setup

Participants wore an EGI HydroCel GSN 256 system (HD EEG with 256 channels) (Tucker, 1993) of appropriate head-size range (figure 2.2). This net had sponges at the electrodes to soak up electrolyte solution (KCl) before application. The net fed into an amplifier station, which was connected to a mac PC installed with a suite of NetStation softwares. This suite was used for both data acquisition and data preparation for analysis (explained in 3rd section).

The participants sat facing the middle of a Microsoft (MS) Surface Hub screen[1] 60cm away in a dark, electrically shielded experiment room (figure 2.2, right side), which was separated from the control room by a partition wall fitted with glass in the centre (figure 2.2(j)). The control room housed control PC installed with E-Prime 2.0, a mac PC for data acquisition from the EEG net, and a network switch to connect control PC to the mac PC. The control PC projected stimulus to MS Surface Hub, simultaneously sending time triggers to the mac PC with trial details. The stimulus for our visual motion study was an animation with 60Hz refresh rate.

Figure 2.1 EGI GSN HydroCel 256 v1.0 (Institut Pasteur, 2013)

[1] Resolution was 1920 x 1080 and screen dimensions were 104.6 cm x 186 cm, for the surface Hub.

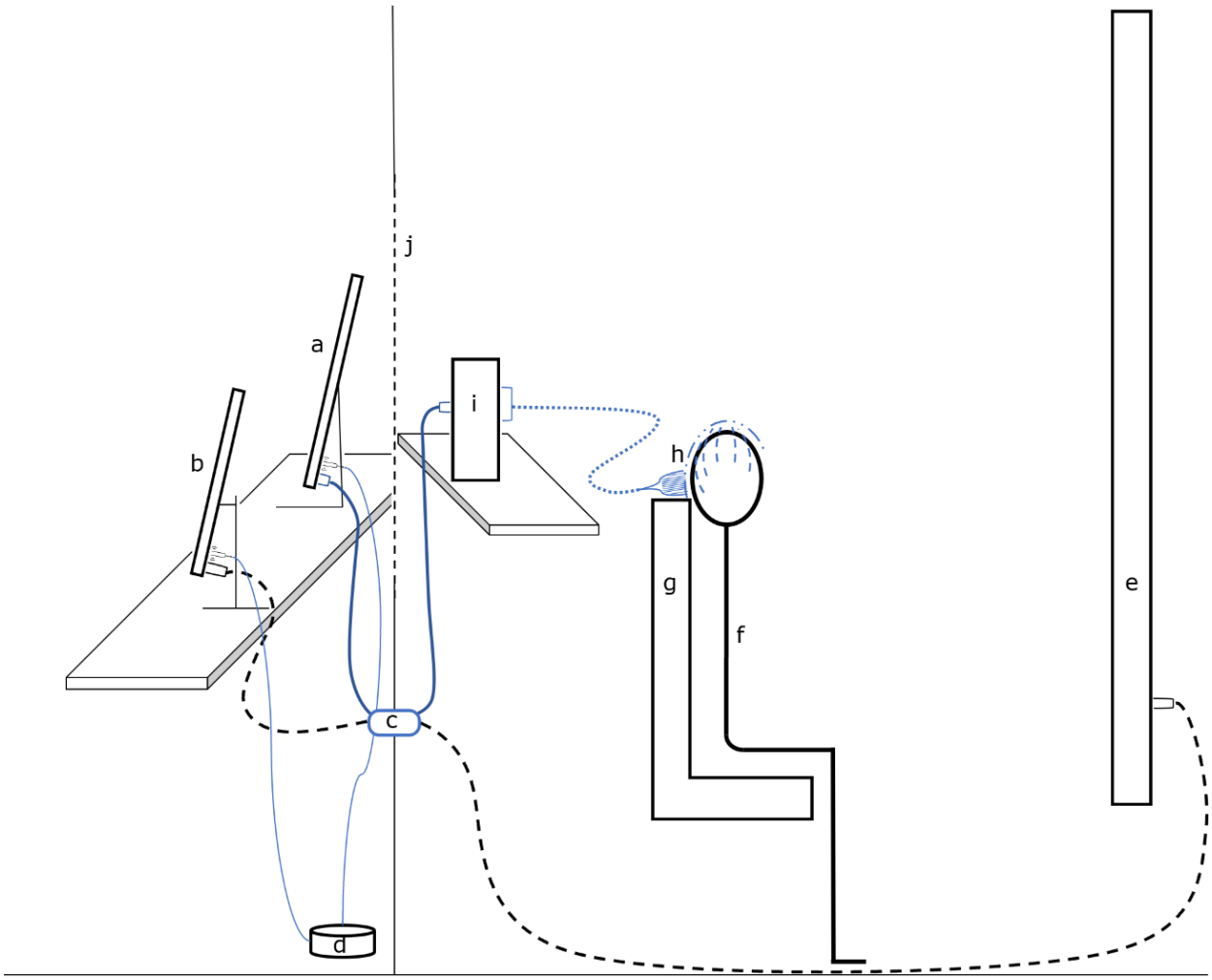

Figure 2.2 Experimental Setup (a) mac PC for data acquisition; connected to amplifier with **thick blue wire**, and to network switch with thin blue wire; (b) control PC for running the experiment; connected to Surface Hub with **dashed black wire**, and to network switch with thin blue wire; (c) hole in the partition wall to allow passage of wires; (d) network switch that connects control PC to mac PC; (e) Microsoft Surface Hub to display stimulus to the participant; connected with control PC with **dashed black wire**; (f) participant; (g) height adjustable chair; (h) EGI HD EEG net; connected with **light blue dotted wire** to the amplifier; (i) amplifier; receives signal from EEG net with **light blue dotted wire**, and sends the signal to mac PC with **thick blue wire**; (j) partition wall with glass shown by dashed line; control room to the left of the wall, experiment room to the right of the wall.

2.1.2 Design

We designed a pinwheel patterned disc with a combination of rotation and looming motion dynamics, to study visual motion perception. (Refer appendix 1a for video link)

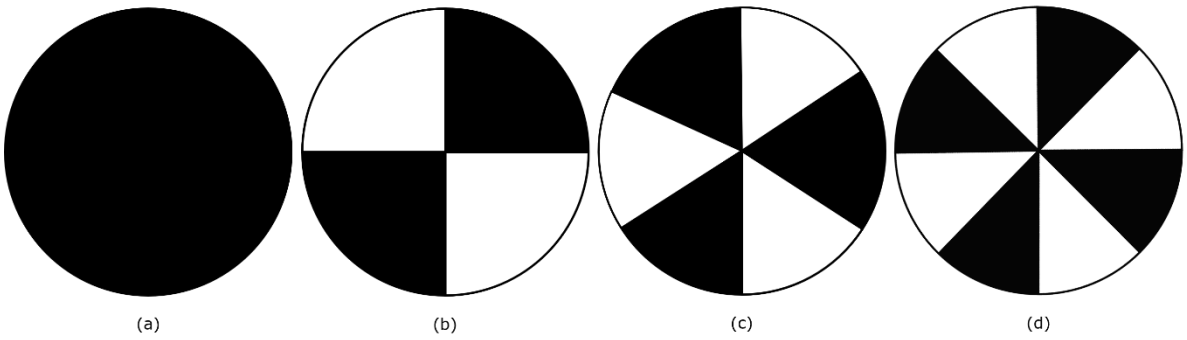

Figure 2.3 Stimulus types (a) Catch Trial/Pie0; (b) Pie2; (c) Pie3; (d) Pie4.

The stimuli were programmed in E-Prime 2.0 on the control PC (figure 2.2 (b)). The program flow structure can be seen in Appendix 1b, and program code is given in Appendix 1c. The stimulus is a 2D projection of a flat disc (or a ball) facing the participant, with a pinwheel pattern on it. This disc loomed towards the participant at a constant acceleration, while rotating at a constant angular speed. The experiment ran for 6 minutes 47 seconds, having 30 trials for each condition, totalling in 120 trials for each participant. The trials had a randomized sequence with no provision to stop repetition of the same stimulus type in consecutive trials. The background colour of the trial scene was light grey (rgb value: 220,220,220). To make the pinwheel pattern, alternate black and white circular sectors were used. The number and angle of these sectors were always equal for all the experimental conditions (figure 2.3). We used four conditions, a catch trial Pie0 (also used as a control condition), three target conditions, Pie2, Pie3, Pie4.

The participants were requested to always look at the centre of the disc. The baseline period helped to fixate gaze. Figure 2.4 (a) helps to understand the visual motion by showing ~1 second window of the total stimulation period for Pie4 condition in 4 snapshots. The red dots and arrow guide visualization of the rotation but are not a part of the actual stimuli.

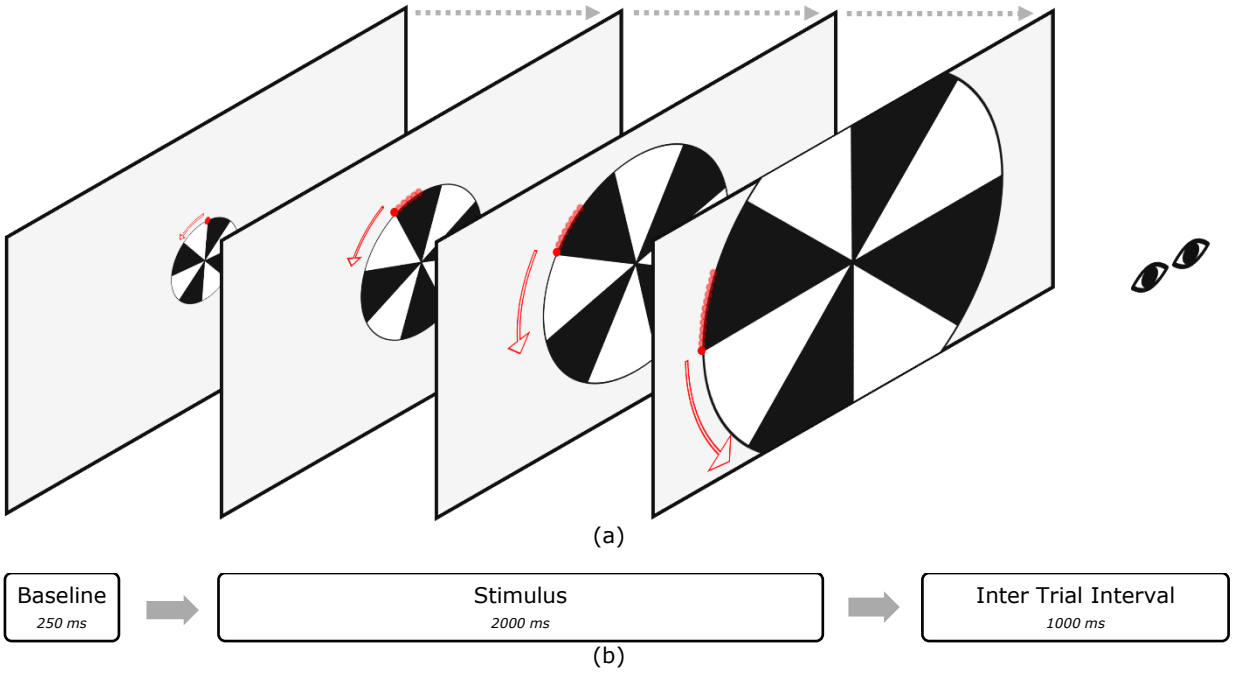

Figure 2.4 Experiment Trial (a) Frame by frame snapshots of stimulus for a ~1 second duration (follow red dot and arrow to visualize rotation, they're absent in the actual stimulus). The participant on the right sees an anticlockwise rotation. (b) Trial breakdown: first a short baseline period, where a projected disc (*loom*) rotates at a fixed distance. Then in stimulus period, the disc takes 2 seconds to loom towards the participant while rotating. It is followed by inter trial interval period displaying completely blank background for 1 second, before the next trial starts.

To visualize how the rotation and looming would look like simultaneously, trajectory of an edge point on the loom was calculated. Figure 2.5 (a) shows the scatter plot for an edge point at the top (red dot in figure 2.4 (a)) on the looming stimuli (positions separated by 10 milliseconds). The x and y axis tell the x and the y coordinates of the red dot respectively.[2] Figure 2.5 (b) zooms into the previous plot. After zooming in, it can be

[2] To understand the positive and negative coordinates, let's look at angular displacement first. With an angular speed of ~96°/second (1.675 radians/second), the final angular displacement is 192° anticlockwise. The x

seen how looming, and rotation occurred simultaneously during the first 1.5 seconds. For the 1.6-2 second period, looming was much more pronounced than rotation.

$$\omega = \frac{\theta}{t} = 1 \cdot 675\ rad/sec$$

$$2.1 \qquad \begin{aligned} &\Rightarrow \boldsymbol{\theta(t) = 1.675 \times t} \ldots (\boldsymbol{i}) \\ &\boldsymbol{x(t) = R(t) \times cos(\theta(t))} \ldots (\boldsymbol{ii}) \\ &\boldsymbol{y(t) = R(t) \times sin(\theta(t))} \ldots (\boldsymbol{iii}) \end{aligned}$$

Equations 2.1 (ii) and 2.1 (iii) govern the relationship shown in figure 2.5 scatter plots. Cosine and sine of angular displacement ($\theta(t)$) control the rotational motion. The radius function ($R(t)$) that varies with time is responsible to control looming motion.

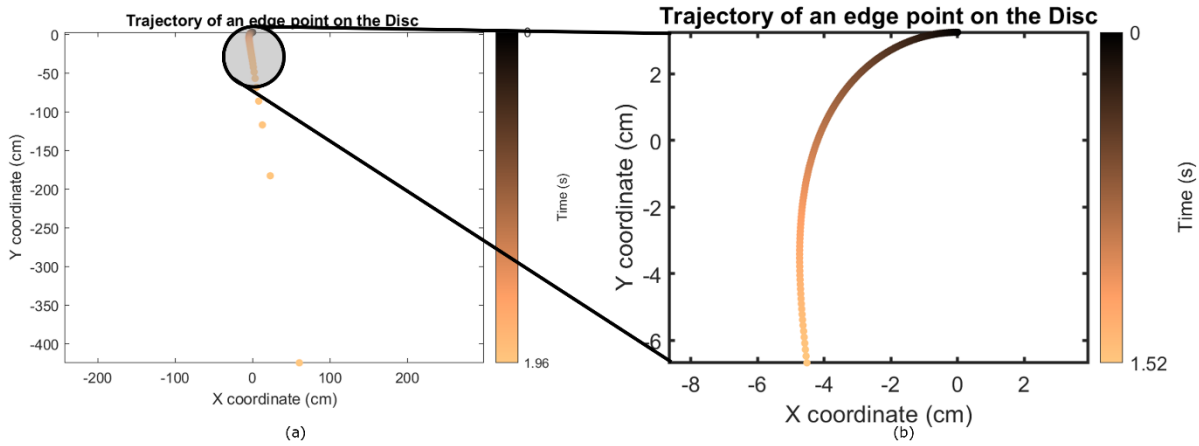

Figure 2.5 Stimulus Trajectory (a) Path followed by a point on top of the edge of the disc during the stimulus period (path of the red dot in figure 2.2). Plot points are 10ms apart. Radius of the disc reaches a maximum value slightly before 2 seconds, because of how the radius of the disc is calculated. This only affects the last frame of the projection and is usually unnoticeable. [3] (b) Zoomed in plot shows path traversed by an edge point for 1.52 seconds. Notice how rotation and looming are both prominent up until 1.52 seconds.

As mentioned earlier, the looming stimuli is a 2D projection of a 3D disc moving towards the participant at a fixed acceleration. This is demonstrated in figure 2.6. Equation 2.2 shows how $R(t)$ is related to the displacement of the real disc.

$$2.2 \qquad \begin{aligned} &\textbf{In figure 2.6, based on similariy of triangles,} \frac{\boldsymbol{R(t)}}{\boldsymbol{x_s}} = \frac{\boldsymbol{R_L}}{\boldsymbol{x(t)}} \ldots (\boldsymbol{i}) \\ &\Rightarrow \boldsymbol{R(t)} = \frac{\boldsymbol{R_L \times x_s}}{\boldsymbol{x(t)}} \ldots (\boldsymbol{ii}) \end{aligned}$$

R_L is the radius of the real disc (65 cm), x_s is the screen distance from participants (60 cm). The stimulus period is 2 second (t_{trial}), distance where the real disc starts is 1200 cm (x_0 to the right of the screen), and the distance where the disc stops is 40 cm (x_{end}, to the left of the screen). R_0 is radius of the disc (projected) at the start when x(t) = x_0, and time is 0. One can calculate using equation 2.2 (i)

---

coordinates are negative since the rotation is anticlockwise, up to 180° (at 1.87 milliseconds) putting the position of x coordinate to the left of origin (starting point for the dot), after which x coordinates become positive, once the dot's position is right relative to the origin. The y coordinate remains negative throughout, as the anticlockwise rotation combined with looming always keep the dot downwards along the vertical direction (negative y axis), relative to the origin.

[3] The last frame of the stimuli suffers from a visual artifact – where a 180° reversal happens due to the sign change in equation 2.5 (ii) after $\sqrt{(120/31)} \cong 1.967$ seconds. However, this artifact is only displayed in the Pie3 condition. 2Pie and 4Pie conditions are not affected by 180° reversal. For Pie3 condition, the effect of the last frame will be after 2 second period, which is not a part of the analysis.

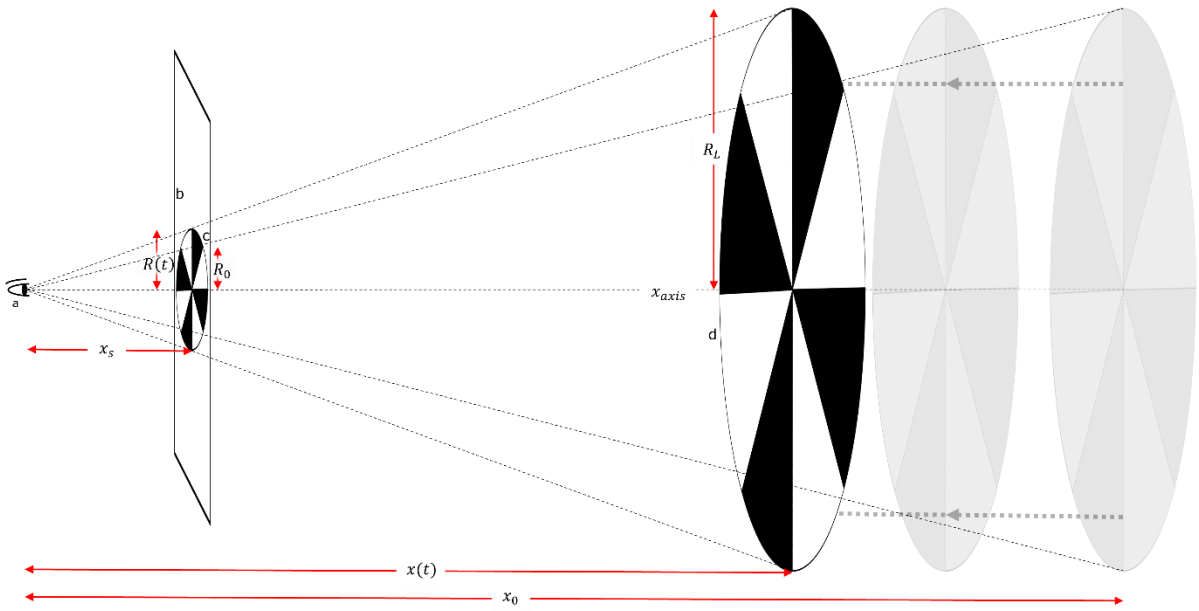

Figure 2.6 Stimulus Projection (a) eye of the participant; (b) screen; (c) disc (projection); (d) real disc or ball. We intend for the real disc (object 'd') to move towards the participant with a constant acceleration. Radius of the projection (object 'c') grows inversely to the distance of the real disc from the screen. Refer equation 2.2 (ii).

$$\frac{R_0}{x_s} = \frac{R_L}{x_0}; \implies R_0 = \frac{65 \times 60}{1200} = 3.25\ cm$$

To calculate x(t) we need to use Newton's equations of motion, as there is a constant acceleration (equation 2.3).

$$2.3 \qquad \begin{aligned} \vec{v} &= \vec{u} + \vec{a}t \ldots (i) \\ \vec{v}^2 - \vec{u}^2 &= 2\vec{a}\vec{x} \ldots (ii) \\ \vec{x} &= \vec{u}t + \frac{1}{2}\vec{a}t^2 \ldots (iii) \end{aligned}$$

In our case, all the vectors are along the x_{axis}, left $(\longleftarrow)$is $-ve$ and right $(\longrightarrow)is +ve$, screen is considered the origin. As $u = 0$, equation 2.3 (i) turns to $v = at$. After transposing, we get:

$$\frac{v}{t} = a \ldots (i)$$

2.4 **Similarly, with u $= 0, \vec{x}$ becomes Δx (displacement in 1D is change in distance),**

$$v^2 = 2a\Delta x \ldots (ii)$$

$$\text{substituting } (i) \text{ in } (ii), v^2 = 2 \times \left(\frac{v}{t}\right) \times \Delta x \ldots (iii)$$

$$\Rightarrow v = \frac{2\Delta x}{t} \ldots (iv)$$

$$v = \frac{2\Delta x}{t} = \frac{2 \times (x_{end} - x_0)}{2 \times t_{trial}} = \frac{2 \times (-40 - 1200)}{2} = -1240\ cms^{-1}$$

$$a = \frac{v}{t} = \frac{1.24}{2} = -620\ cms^{-2}$$

In equation 2.3 $(iii), \vec{x}$ becomes Δx (in 1D), $\quad u = 0, \quad x(t) - x_0 = \frac{1}{2}at^2$

2.5 $$\implies x(t) = x_0 + \frac{1}{2}at^2 = 1200 + \frac{1}{2} \times (-620)t^2 = 1200 - 310t^2 \ldots (i)$$

substitute (i) in equation 2.2 (i) to get, $R(t) = \frac{R_L \times x_s}{(1200 - 310t^2)} = \frac{65 \times 6}{(120 - 31t^2)} \ldots (ii)$

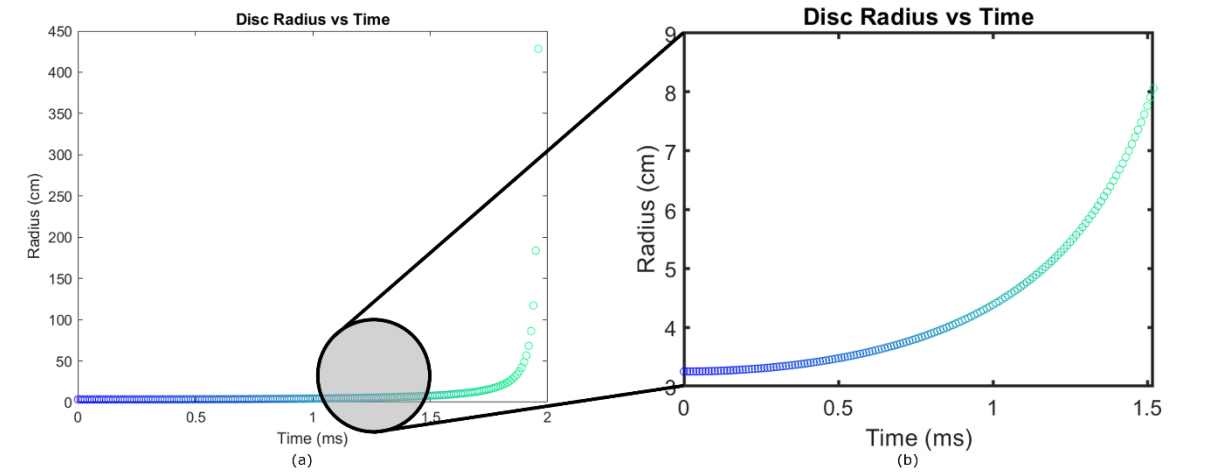

Figure 2.7 Stimulus Radius (a) Relationship between the radius of the disc (loom) until 1.96 seconds. Note how rapidly the radius increases towards the end of the stimulus. (b) Radius of the disc with respect to time until 1.52 seconds. These plots are based on equation 2.5 (ii).

2.1.3 Perceptual Information

To find the relationship between the frequency related feature in the stimulus (at the ecological scale), and the neural dynamics, we had to quantify the motion dynamics of the stimuli used in this study in terms of frequency.

Rotational dynamics were used to obtain perceptual information[4]. Rotation is understood as the motion of a rigid body (a body that doesn't change shape) about an axis passing through itself. Spinning is a case of rotation when the axis passes through the geometrical centre (or centre of mass) of the rigid body. The rate of spinning or rotation is characterized by $\vec{\omega}$, analogous to linear velocity vector $\vec{v}$. The change in position of any point on the rigid body would be the angular displacement $\vec{\theta}$, an analogue to linear displacement $\vec{x}$. Therefore, angular velocity $\vec{\omega} = \frac{\vec{\theta}}{t}$. The angular velocity can also be understood as angular frequency – rate of rotation (in radians) per unit time (second).

In this study, angular velocity was constant across all 3 conditions. The differentiating factor between conditions was the number of circular sectors.

In figure 2.8, if one starts (red dot) rotation along the arrow, and stops where it ends (light blue dot), then

- in figure 2.8 (a) Pie2 will rotate by π radians and return to original orientation.
- in figure 2.8 (b) Pie3 will rotate by $^{2\pi}/_{3}$ radians and return to original orientation.
- in figure 2.8 (c) Pie4 will rotate by $^{\pi}/_{2}$ radians and return to original orientation.

When a disc returns to its original orientation, then it becomes visually indistinguishable from its starting position.

If θ_{Pie} is the angular displacement of any experimental condition to return to the original orientation, and t_{Pie} is the time taken to complete that displacement, then

[4] At this point, one might wonder, why have looming at all? High ecological validity in an optical flow situation (which inevitably happens when a person approaches/walks up to/drives up to, a rotating object to examine it). Perceiving any rotating object while moving, would be represented by these stimuli.

$$\frac{\theta_{Pie}}{\omega} = t_{Pie} \dots (i)$$

$$2.6 \quad \Rightarrow \frac{\omega}{\theta_{Pie}} = \frac{1}{t_{Pie}} = f_{Pie}{}^{5} \dots (ii)$$

$$As\ \omega = 1.675\ \text{rad}\, s^{-1},\ f_{Pie2} = \frac{1.675}{\pi} = 0.53316\ Hz$$

$$f_{Pie3} = \frac{1.675}{\left(\frac{2\pi}{3}\right)} = \frac{1.675 \times 3}{2\pi} = 0.799753\ Hz$$

$$f_{Pie4} = \frac{1.675}{\left(\frac{\pi}{2}\right)} = \frac{1.675 \times 2}{\pi} = 1.06633\ Hz$$

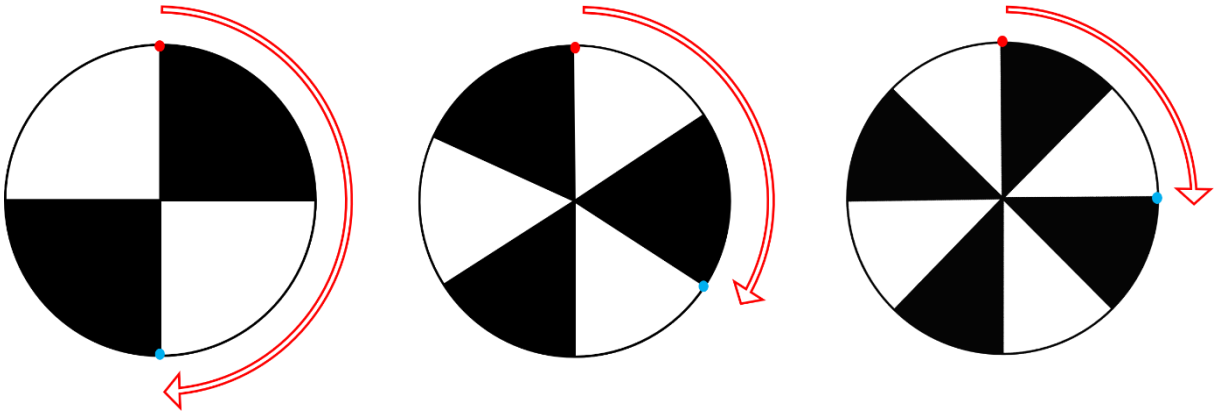

Figure 2.8 Perceptual Information (a) Pie2 rotates 180°, (b) Pie3 rotates 120°, and (c) Pie4 rotates 90°, before all return to the identical orientation. (Follow the start dot, end dot and arrow to visualize rotation)

If t_{Pie} is the time taken to complete the minimum angular displacement to return to the original orientation, then f_{Pie} is the number of times a disc projection returns to its original orientation in unit time (1 second).[6]

Since there was a catch trial with no pattern (figure 2.3 (a)), which was used as a control in TSE calculation, ERD/S resulting from purely looming were subtracted from the 3 experimental conditions, leaving behind the brain activity arising from rotation. [7]

2.2 Participants

12 participants (7 males) in the age group of 22 – 31 years (mean = 25.42, SD = 2.47) were recruited for this study. They were allowed to participate after signing a consent form (appendix 1d). The participants had to fill a handedness test (Edinburgh

[5] One must not confuse f_{Pie} with the frequency in $\omega = 2\pi f$, which is used for a sinusoidal function.

[6] One might even think that instead of varying the pinwheel pattern across condition it might be a better experimental design to vary the angular velocity (low, high etc). For spherical and circular objects in the real world, we perceive rotation only when there are textures or patterns on the surfaces of the rotating and spinning bodies. Take for instance a frisbee – if it is perfectly smooth, evenly coloured, then it is quite hard to see it spinning once launched. If at all the spinning is visible, it would be because of the uneven scattering of light, partial reflection at the frisbee's surface or multiple light sources allowing different amounts of scattering/diffused reflection. If on the other hand the frisbee has a pattern on it (that is distinguishable while rotation), then it's quite easy to perceive rotation.

[7] It might seem that we are trying to separate looming and rotation in a convoluted manner. However, a rotation in optic flow has never been analysed. Only pure rotation has been studied by Kleinschmidt et. al (2002) in the MRI study.

handedness inventory) and answer questions pertaining to gestational period and video game experience. There were no filter criteria applied to select the participants. This study was conducted under a prior approval sought from the regional committee for medical and health research ethics.

2.3 Data

Data was acquired using EGI's GSN HydroCel 256 v1.0 EEG system (figure 2.9). This net has 256 channels and a separate electrode (top position of the head) served as a common reference channel (v_{ref}).

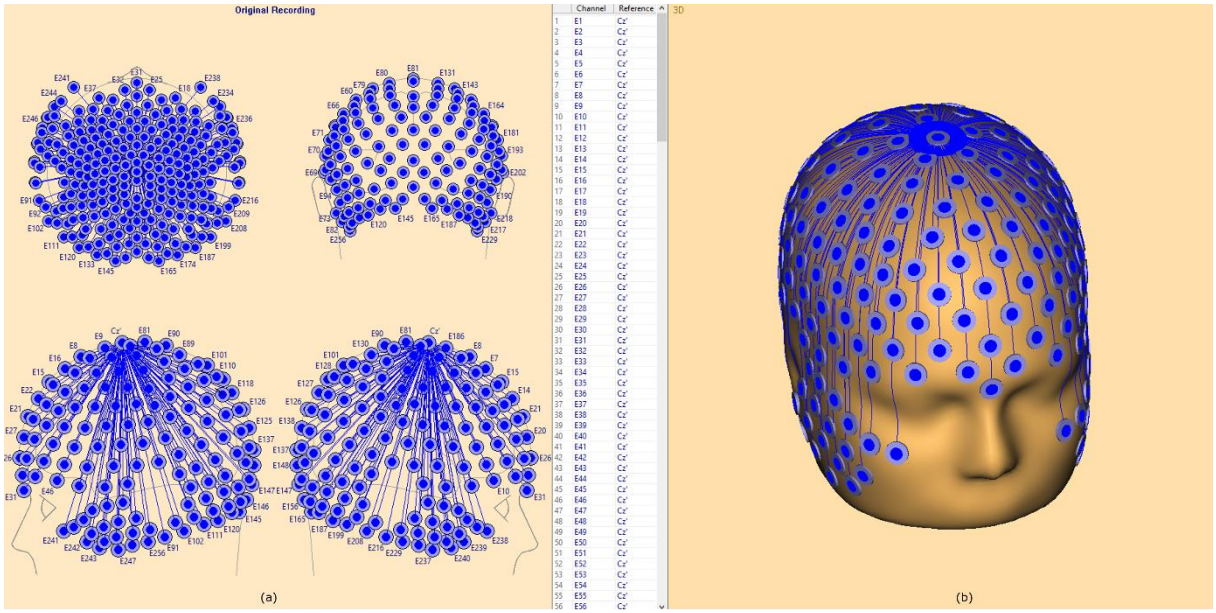

Figure 2.9 HD EEG layout (a) *clockwise:* top, rear, right side, left side view; (b) 3D model

2.3.1 Acquisition

The electrode impedance was visually monitored with NetStation 4 on the mac PC inside the control room, right before the experiment. Electrode sponges were dripped with electrolyte and shifted to fit snugly on the scalp if the impedance for any electrode exceeded 50 kiloohm (Ferree, Luu, Russell, & Tucker, 2001; Picton et al., 2000). Once most of the electrodes showed impedances under 50 kiloohm, the experiment was started.

The timeseries EEG data was acquired at a sampling rate of 500Hz, bandpass filtered from 0.1Hz to 200Hz with NetAmp 400 amplifier on NetStation 4 acquisition software. The data was saved in metafile format (.mff) by NetStation 4 acquisition.

Once the experiment was over, we had to markup EEG recording for use in BESA 7.0 with NetStation 5 Tools software.[8] It allowed creation of manual triggers (time labels) by use of rule-based statements as one of the functions under segmentation option. For instance, every trial's stimulus period begins with *stm+* trigger, and each trial has a trial specific (*TRSP*) event marker containing information sent by E-Prime 2.0.[9] So, a rule would be *'when trigger is stm+* ***&*** *keylabel for the condition is Pie0→ new trigger is* ***Pie0****'*.

[8] BESA recognizes only the time triggers. TRSP information is not visible in the raw files converted from the .mff format. To help label each trial with the correct condition, segmentation markup is needed.

[9] This information is a spreadsheet containing the three different conditions and their respective variables, and identifiers in a *keylist*.

Similarly, for Pie2, Pie3 and Pie4 conditions. The segmented data is then exported to .raw format from the default .mff format, in the same software.

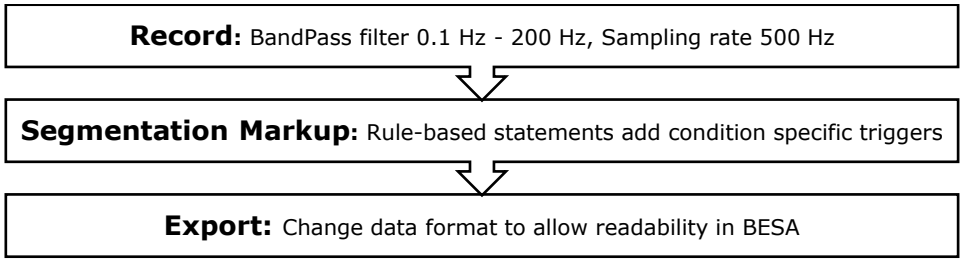

Figure 2.10 Data Recording flowchart

2.3.2 Pre-processing

A.C. electricity caused line noise (50Hz) to creep in the recorded data. To handle the line noise, notch filter of 50Hz with a 2Hz width was used in BESA 7.0. Low cut-off value of 1.6Hz (zero phase 12dB) was chosen for high-pass filter to remove drift due to D.C. current and lower frequency components. A low-pass filter with cut-off value of 100Hz (zero phase 24dB) was chosen to ensure less attenuation at 50-60Hz. Filter response can be understood in figure 2.12.

Bad electrodes were marked, and dead electrodes and electrodes with minor fluctuations were interpolated (see results for exact numbers) using spherical splines interpolation method (Perrin, Pernier, Bertrand, & Echallier, 1989; Picton et al., 2000). (BESA's artifact scan tool was used to reject trials allowing the highest amplitude = 200 microvolts, the highest gradient = 75 microvolts, and the lowest permissible amplitude = 0.1 microvolts. Blink artifact was removed using BESA 7.0 automatic blink removal feature. It made use of an internal topographical model to search for instances of blinks, and then used principal component analysis (PCA) to remove blink artifact from the entire data (Berg & Scherg, 1994; Ille, Berg, & Scherg, 2002). Trials with movement artifacts were manually removed with visual inspection.[10]

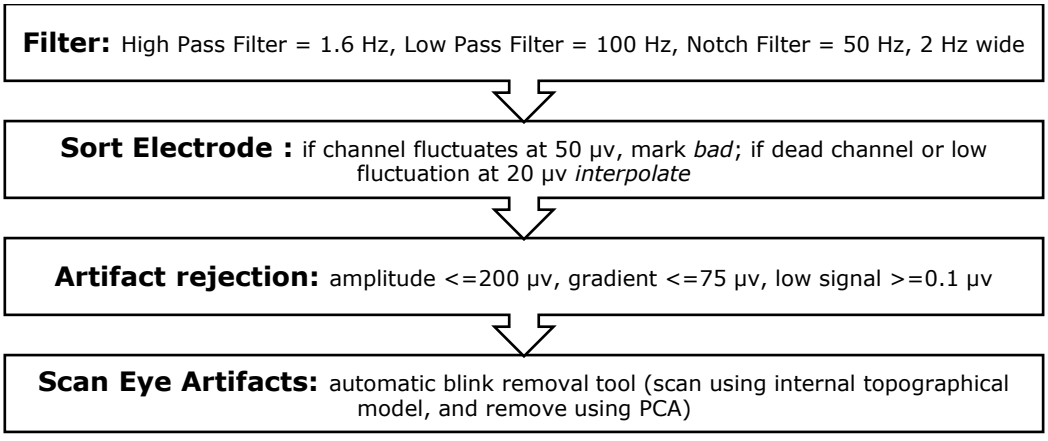

Figure 2.11 Data Pre-processing pipeline

[10] A note on handling artifacts. Manual artifact removal is quite subjective process. Since it is an exploratory study, removing artifacts introduces unknown biases. Automatic artifact removal pipelines could be used, however, there is no guarantee that they won't end up eliminating meaningful signals misinterpreted or intertwined with artifacts.

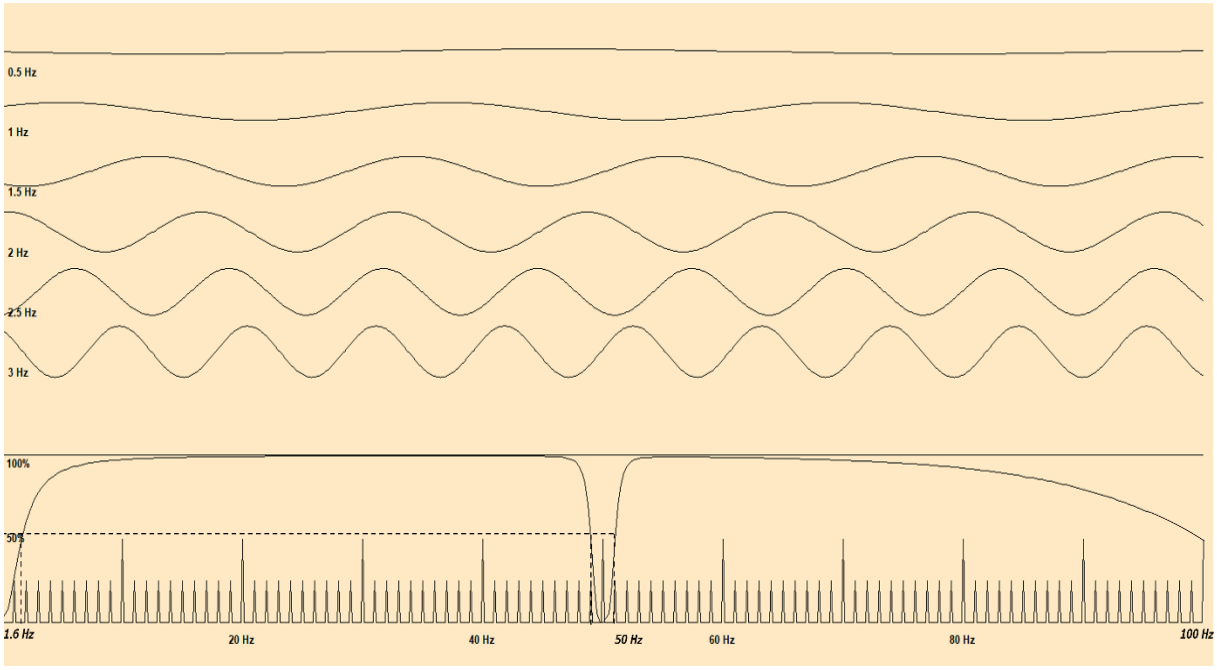

Figure 2.12 Filter Response 1.6Hz High-pass filter, bottom-left; 50Hz notch filter 2Hz wide, bottom-middle; 100Hz Low-pass filter, bottom-right. *Top part* shows attenuation of the respective sinusoidal waves from 0.5 – 3Hz, with 0.5Hz step size. 0.5Hz and 1Hz sine waves are the most attenuated and appear almost flat. 1.5Hz sine wave is attenuated roughly 50% (see also at bottom left, 50% amplitude at 1.6Hz). *Bottom part* shows amplitude curve with frequencies from 0-100Hz. Observe how amplitude is 50% at the exact frequency cut-offs.

2.4 Analysis

Analysis was carried out in the time-frequency domain, in VEP source montage, a default montage in BESA 7.0. Image compositing was used to discover trends across average participant sample, and FFT of TSE bands of specific source channel was calculated for individual participant analysis.

2.4.1 Source Montage

A source montage applies inverse spatial filters to separate brain activity using a multiple source model calculated from EEG data. This montage had precalculated source dipoles at 17 locations (referred to as source channels in TSE plots) (Scherg et al., 2002). The visual cortex had 7 single dipoles with specific orientation and location, rest of the brain sources were depicted by 10 regional sources with specific locations. For this study, only the visual cortex sources were studied.

The naming convention used for the source channels is given in table 2.1.

Table 2.1 Nomenclature for Source channels

VC, Fp, F, TA, C, P	**Visual Cortex, Fronto-polar, Frontal, Temporal Anterior, Central, Parietal**
r, b, l, v	**r**adial, **b**asal, **l**ateral, **v**ertical
L, M, R	**L**eft, **M**iddle, **R**ight

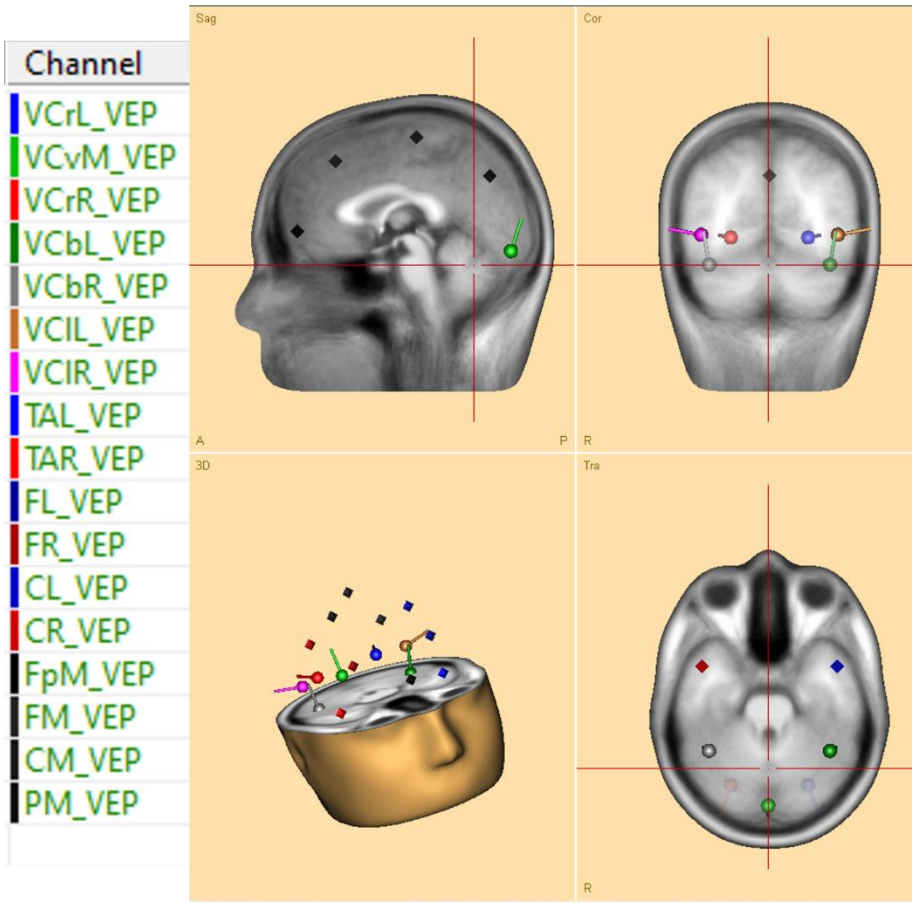

(a)

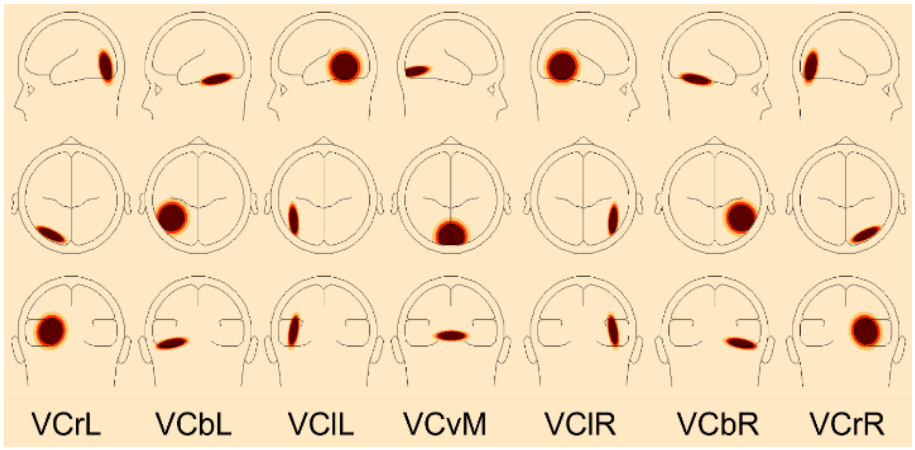

(b)

Figure 2.13 Source Locations (a) VEP source montage includes 17 source channels in BESA; (top left, clockwise) Sagittal, coronal, transverse, and 3D views. 10 are regional sources (with only location– diamonds ♦), 7 are single dipoles (with location and orientation – lollipops ●—). (b) 7 Visual cortex single dipoles (top to bottom) side, top, rear views; for each dipole, orientation is perpendicular to disc.

2.4.2 Time Spectral Evolution

Time spectral evolution is a relative measure of brain activity in time-frequency domain, that gives normalized amplitude values compared to the baseline period. We used complex demodulation (Granger, Hatanaka, 1964) with suitable temporal resolutions to calculate TSE in this study. TSE was calculated by first converting each trial (with time-series data) to time-frequency domain with complex-demodulation, then taking an average of amplitude across trials. Finally, the amplitudes in stimulus period (0-2000ms)

were normalized with respect to the baseline (-250-0ms). Following expression is a general representation of a time-frequency transformation.

$$S_n(f,t) = A(f,t) \times e^{i\phi(f,t)}$$

S_n is the time-frequency domain signal. A(f,t) represents amplitude and the exponential term represents the phase. Following equation shows the formula used for TSE calculation.

$$TSE = \frac{A(t,f) - A_{baseline}(f)}{A_{baseline}(f)} \times 100\%$$

$$A(t,f) = t$$

$$A_{baseline}(f) = mean$$

A(t, f) stands for activity at time t and frequency f (either power or absolute amplitude)
A baseline(f)is the mean activity at frequency f over the baseline epoch.
The TSE value is in the range from [– 100 %, +100%] and describes the spectral change of activity at sampling time t relative to the activity during the baseline epoch.
A value of + 100% means that activity is twice as high as during the baseline epoch

Regression analysis was used to separate evoked activity from induced activity by accounting for fluctuations between trials. Probability maps were calculated to find significant values in TSE plots using bootstrapping statistics. This is a non-parametric method defined in Davidson, Hinkley (1999).

TSE was compared for a target vs control condition, by simple subtraction after reshuffling of trials. The probability for target vs control condition was performed by a two-sided permutation test, building up on the bootstrapping statistics, to check if the target condition has significantly higher or lower values compared to the control condition.

Event related desynchronization (ERD) is the negative value (in blue) in a TSE plot, and event related synchronization (ERS) is a positive value (in red) in a TSE plot.

2.4.3 Image compositing

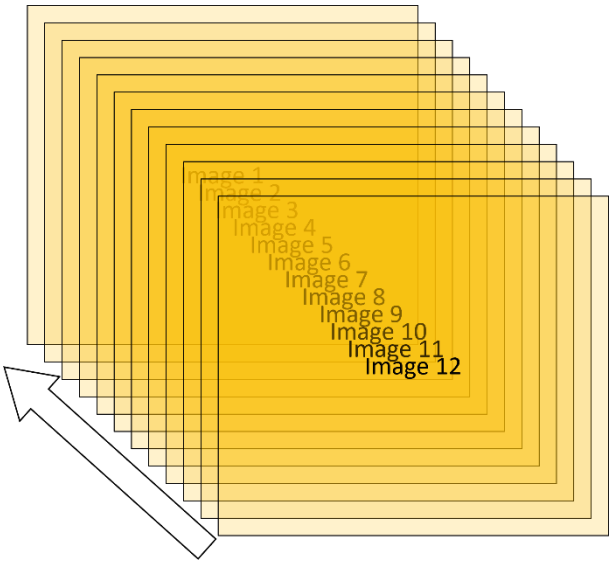

Figure 2.14 Image Compositing 12 images stacked on top of each other for each condition for all 12 participants. It is similar to how one would stack 12 physical transparencies on top of each other.

TSE plot images were stacked on top of each other programmatically in python to calculate an average pixel value and generate a composite image to find trends and patterns in ERD.

2.4.4 Fast Fourier transform

The flowchart in figure 2.15 gives an overview for the individual based analysis of EEG.

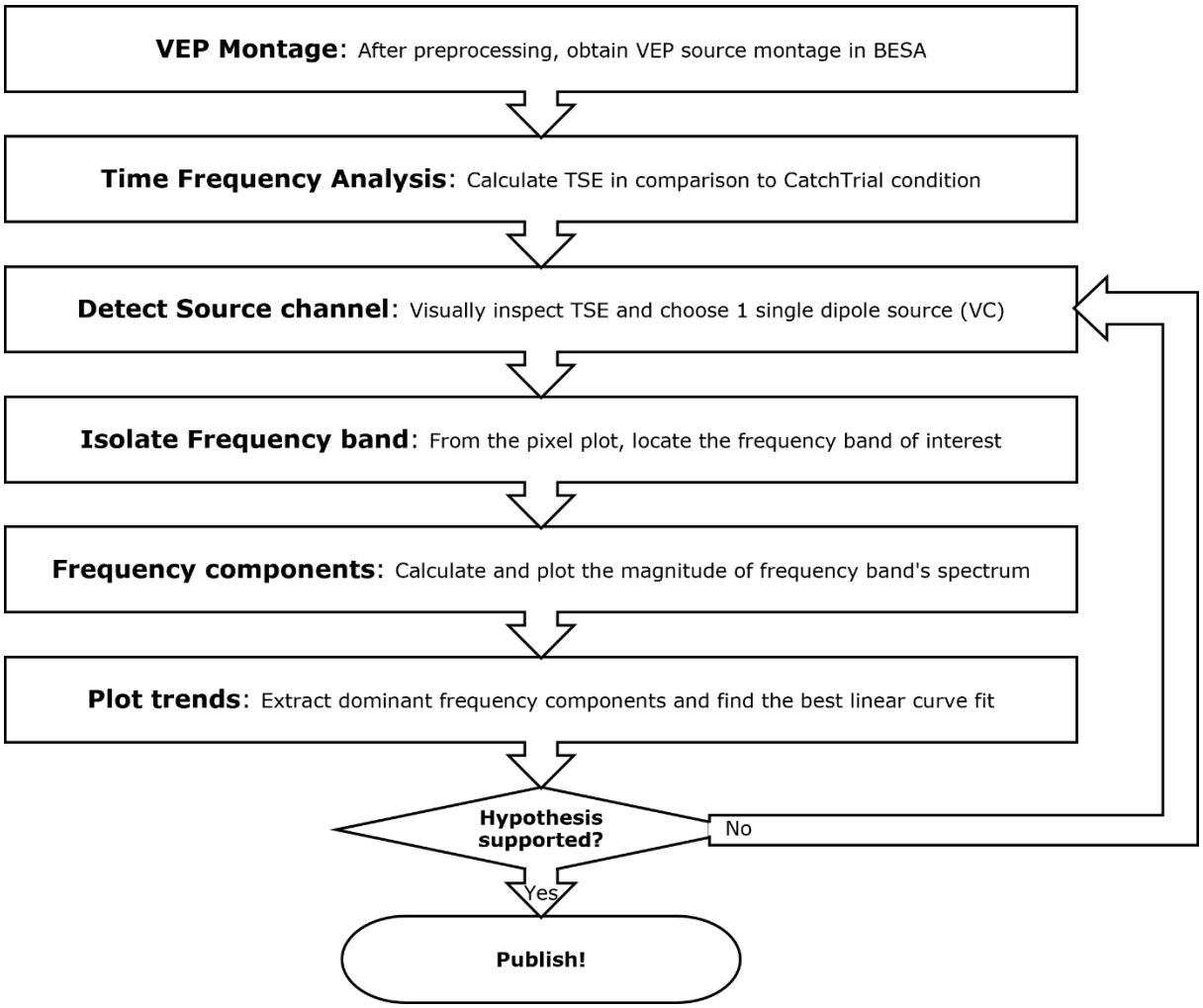

Figure 2.15 Analysis Flowchart

To do an analysis at the individual level, TSE bands of interest were found in specific source channels, which were then subjected to FFT calculation to find distinct frequency components across three comparison conditions (Pie2-Pie0, Pie3-Pie0, Pie4-Pie0). Probability maps were calculated without regression to narrow downs source channels of interest having significant ERD.

The average TSE plot values generated by BESA 7.0 for each participant were exported to MATLAB 2022b.[11] A pixel plot (without contours) for specific source channel was first visually inspected to find relevant frequency band with sustained ERDs. Afterwards, these

[11] BESA shows only contour maps for TSE plots.

frequency bands were extracted and their spectral magnitudes were calculated with FFT formula shown below (Frigo, Johnson, 1998).

$$Y(k) = \sum_{j=1}^{n} X(j) W_n^{(j-l)(k-1)}$$

X is the function of j (time), whose FFT needs to be calculated.

Y is the function in k (frequency) which is computed after transformation.

$W_n = e^{(-2\pi i)/n}$, is the root of unity, carrying the phase component information.

2.4.5 Curve fitting

After obtaining values for the frequency components from FFT, 3 frequencies for each target vs control condition were plotted with the respective return to orientation frequency value for each stimulus. MATLAB's curve fitting toolbox was used to fit a line on these three plot points for each participant. Four parameters were calculated to estimate the goodness of fit statistics. Sum of squares due to error (SSE) gave the total deviation of the plot points from the predicted points on the line (closer to 0 is a better fit). Square of the correlation (R-square) between the plot values and the predicted values was calculated to indicated what percentage of variation of the data around the average was explained by the linear model (closer to 1 or 100% is better). Adjusted R-square statistic is a modified R-square value (closer to 1 or 100% is better). Root mean square error (RMSE) was calculated to find the standard error of regression.

3 Results

This section first shows the typical approach for EEG studies, where characteristics obtained from analysis (TSE in our case) were studied by averaging across participants. This approach did not help to establish any compelling evidence for ecological resonance. In the next section, a new approach to analyse TSE data was attempted for 2 participants with the least noisy data, individually. This approach presented strong evidence to support our hypothesis.

3.1 Average TSE across participants

1118 trials were accepted out of 1440 trials in total. Mean trials accepted across participants was 93.16 and SD = 21.54. TSE plots for all participants were calculated for 7 different situations. 4 situations arose out of the 3 (single) experimental conditions and 1 catch trial, when no control was used (section 3.1.1). 3 more situations arose, when the catch trial was used as a control for TSE calculation (section 3.1.2). Baseline period started 200ms before the stimulus period began. Resolution for TSE was set at 1Hz, 50ms with frequency output varying from 2Hz – 60Hz.[12] TSE plots, as well as probability maps of these TSE calculations were both calculated and composited (see Appendix 2a for TSE plot composites). Probability maps were favoured for analysis because of significant values ($p<0.05$).

3.1.1 No-control condition

VCrL (visual cortex radial left) source channel in Pie0, Pie2, Pie3, and Pie4 TSE probability maps, showed significant ERD ($p<0.05$) in 8Hz band. For Pie0, Pie2, Pie4 8Hz had significant ERD from 0-2000ms. For Pie3, the significant ERD was from 200-2000ms. The lower-bound frequency bands were 6Hz, 7Hz, and 8Hz for Pie2, Pie3, Pie4 conditions respectively, whereas the upper-bound was 12Hz. Pie3 had ERD components in 11-12Hz band as well, although unlike Pie2 and Pie4, Pie3's ERD occurred in long discontinuous bursts. Pie2 and Pie4 had the same upper-bound frequency band of 12Hz. Pie4's 4Hz band had regularly spaced bursts of ERD activity, with a spacing of 200ms up until 1 second, and then 400ms up until 2 second.

In *VClL (visual cortex lateral left)* channel, all 4 conditions had ERD in 8Hz frequency band. Pie0 had short bursts of ERD regularly spaced by 400ms. Pie2 and Pie4 had 3 long bursts of ERD with irregular latencies and different time durations. Pie3 had a continuous ERD from 0-2000ms. Pie0 and Pie3 both had sustained ERD until the end (2000ms) in 12Hz frequency band. However, Pie0's 12Hz ERD started late at 1100ms, and Pie3 started at beginning (0ms). Pie0, Pie2, and Pie4 had ERD in 18Hz frequency band. ERD latencies overlapped for Pie0 and Pie2 at 200ms and 1200-1400ms. ERDs overlapped for Pie0 and Pie4 at 900ms in 18Hz band. No time overlaps were found for all four taken together in the 18Hz band.

Upon inspecting *VCrR (visual cortex radial right)* channel, 12Hz frequency bands were found to be across all 4 conditions, sharing latencies for ERDs at 200ms, 500ms, 700ms

[12] This resolution was chosen because it allowed the separation of frequency bands to a narrow window of 1 Hz. Which in turn allowed to search for frequency bands specific to the experimental conditions, in tune with research objective number 2.

and 1400ms. Pie3 had no other distinguishing frequency band. Pie0, Pie2, Pie4 also shared ERDs in 6Hz band at 400ms, 800ms, 1600ms, 2000ms. Between Pie2 and Pie4, Pie4 had all the components of Pie2 (6 – 8Hz, 9 – 12Hz) as well as extra components at 22Hz.

VCbL, VCvM, VCbR, VClR channels did not have enough significant values in the probability maps to observe trends.[13]

Table 3.1 Observation for TSE Probability map no-control condition

TSE / SOURCE	Pie0	Pie2	Pie3	Pie4
VCrL	8Hz → 0 - 2000ms	6-12Hz → 0 - 2000ms	7-8Hz → 200 – 2000ms 11-12Hz → 0-700ms, 850 - 1250s, 1350 – 1700ms, 1850 – 2000ms	4Hz → 400ms, 600ms, 800ms, 1000ms, 1400ms, 1600ms, 2000ms 8-12Hz → 0 – 2000ms
VCbL	Inconclusive	12Hz → 200-500ms, 850ms, 1100ms, 1400ms, 1800ms 16Hz → 200ms	10-11Hz → 200ms, 1000ms, 1800ms 18Hz → 400ms, 1800ms	9Hz → 50 - 550ms, 850 – 1050ms, 1600 – 2000ms 15Hz → 300 - 450ms, 800 - 1100ms, 1200 - 1500ms, 1700 – 2000ms
VClL	8-9Hz → 400ms, 800ms, 1200ms, 1600ms 12Hz → 1100 – 2000ms 18Hz → 200ms, 900ms, 1200 -1400ms	8-9Hz → 100 - 700ms, 900 - 1200ms, 1500 - 1900ms 17-18Hz → 0 – 200ms, 800ms, 1200 – 2000ms	8-10Hz → 0-2000ms 12-14Hz → 0 – 2000ms 15Hz → 0-150ms 16Hz → 0-150ms, 1200 – 2000ms	4Hz → 500ms, 700ms, 1100ms 8Hz → 300 – 500Hz, 1250 – 1700ms, 1800 – 2000ms 10-11Hz → 400ms, 600ms, 1000ms, 1650ms, 1900ms 18,20Hz → 900ms
VCvM	Inconclusive	Inconclusive	Inconclusive	Inconclusive
VCrR	6Hz → 400ms, 800ms, 1200ms, 1600ms, 2000ms 12Hz → 200ms, 500ms, 700ms, 1400ms, 1700m	6-8Hz → 0 – 600ms, 750 – 1200ms, 1300 – 2000ms 9-12Hz → 0 – 2000ms	12Hz → 0-300ms, 500-700ms, 900ms, 1200-1400ms	6-8Hz → 250 – 2000ms 9-12Hz → 0 – 900ms, 1400ms, 1600 – 2000ms 22Hz → 1400 – 1800ms
VCbR	8Hz → 400ms, 1600ms	Inconclusive	16Hz → 300ms, 1900ms	Inconclusive
VClR	Inconclusive	6-10Hz → 0-600ms, 750ms, 950ms, 1500ms, 2000ms 14Hz → 300ms, 600ms, 900ms, 1200ms, 1600ms, 2000ms	10Hz → 200 – 450ms 12Hz → 1300ms	10-12Hz → 50 – 2000ms 20Hz – 450ms, 1150ms, 1750ms

[13] VCbL did not have substantial data for Pie0, so all 4 conditions couldn't be compared. However, Pie2, Pie3, Pie4 each had different frequency bands with ERD. Probability map for VCIR was inconclusive in Pie0 condition, however, 10 Hz band was common across Pie2, Pie3, Pie4 conditions with ERD, at the same time, each condition had a different upper-bound frequency band with ERD.

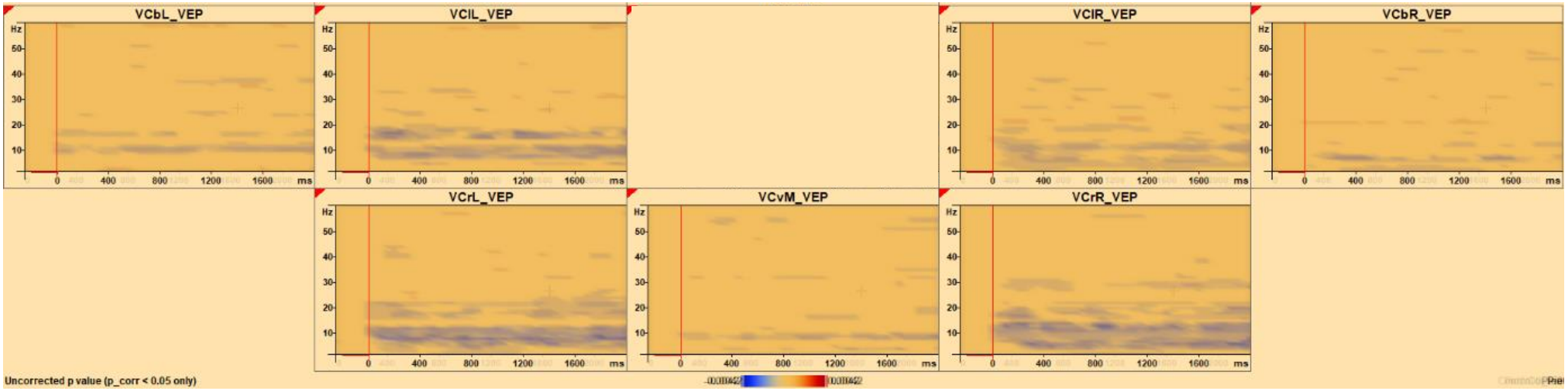

Figure 3.1 Pie0 Composite Image: TSE Probability Map This image was generated by averaging the pixel values of the 12 participants' overlaid images. The plots show significant ($p<0.05$) ERD and ERS in blue and red respectively. Single dipole source channels belonging to visual cortex were considered for analysis. VCbl, VCvM, and VClR channels are inconclusive. VClL, VCrL, VCrR, and VCbR channels show noticeable average brain activity.

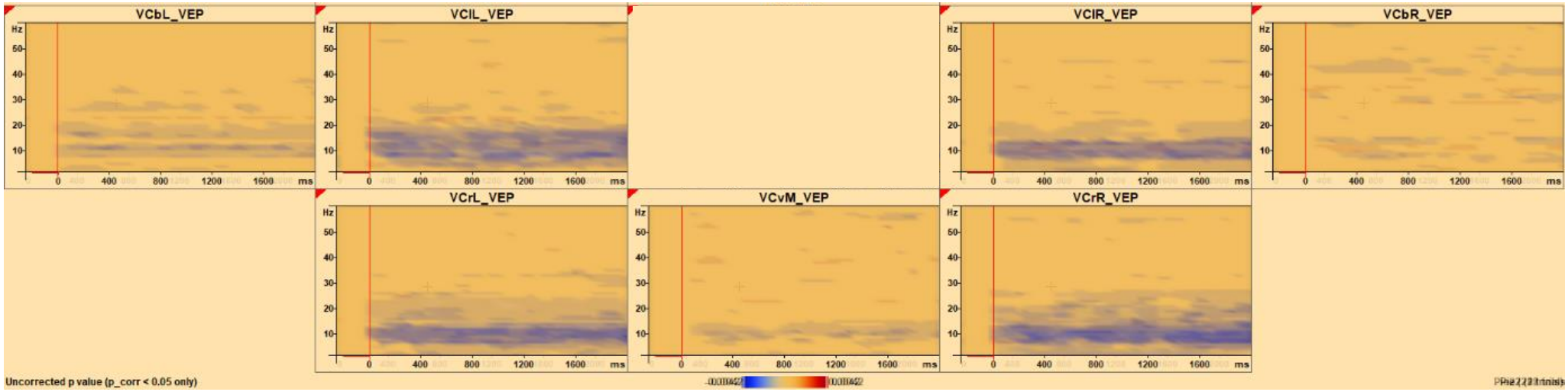

Figure 3.2 Pie2 Composite Image: TSE Probability Map This image was generated by averaging the pixel values of the 12 participants' overlaid images. The plots show significant ($p<0.05$) ERD and ERS in blue and red respectively. Single dipole source channels belonging to visual cortex were considered for analysis. VCvM and VCbR channels are inconclusive. VCbL, VClL, VCrL, VClR, and VCrR show noticeable average brain activity.

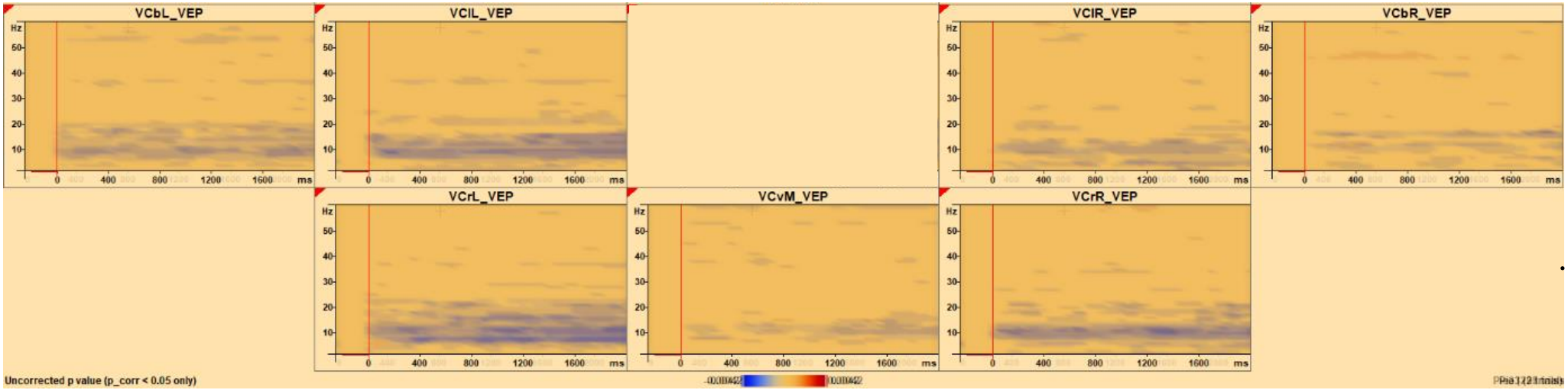

Figure 3.3 Pie3 Composite Image: TSE Probability Map This image was generated by averaging the pixel values of the 12 participants' overlaid images. The plots show significant ($p<0.05$) ERD and ERS in blue and red respectively. Single dipole source channels belonging to visual cortex, were considered for analysis. VCvM is inconclusive. VCbL, VClL, VCrL, VCrR, VClR, and VCbR show noticeable average brain activity.

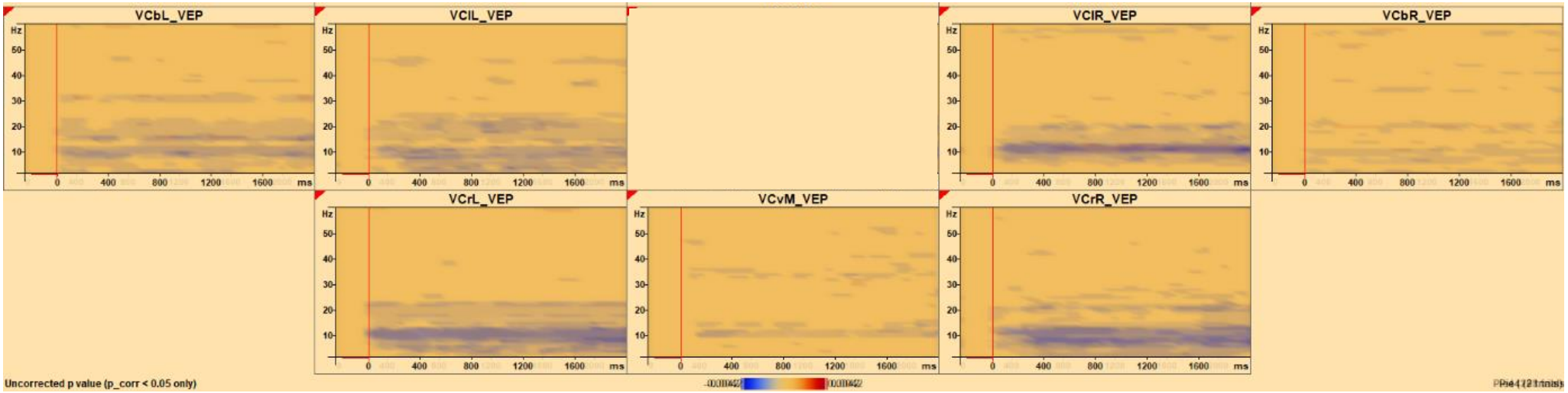

Figure 3.4 Pie4 Composite Image: TSE Probability Map This image was generated by averaging the pixel values of the 12 participants' overlaid images. The plots show significant ($p<0.05$) ERD and ERS in blue and red respectively. Single dipole source channels belonging to visual cortex, were considered for analysis. VCvM and VCbR are inconclusive. VCbL, VClL, VCrL, VCrR, and VClR show noticeable average brain activity.

3.1.2 Target-vs-control condition

The experiment was designed with a catch trial, that could be used as a control for TSE calculation, if the no-target conditions didn't yield compelling evidence. TSE for the 3 conditions Pie2-Pie0, Pie3-Pie0, and Pie4-Pie0, were calculated and the plot images were stacked on top of each other to obtain composites in figure 3.5 – 3.7.[14] Appendix 2b gives the TSE plot composites for the three *target vs control* conditions.

The composites did not reveal trends for average brain activity across participants. This suggested that the *target vs control* conditions contained characteristics that differed on an individual level for each participant.

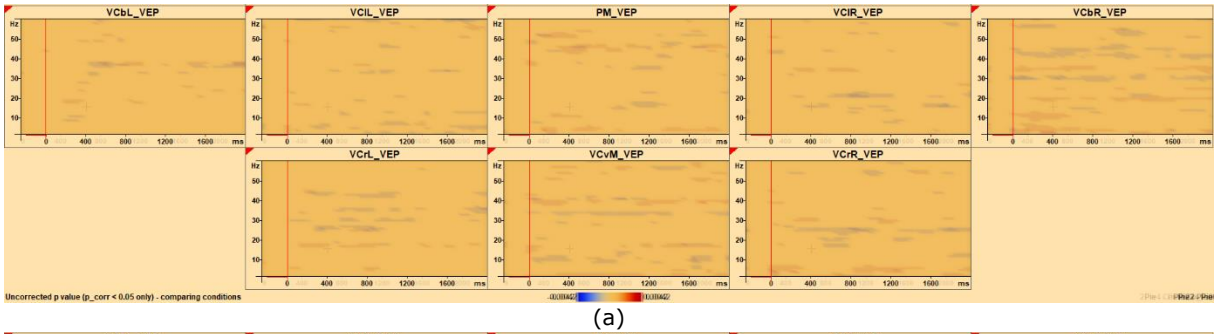

(a)

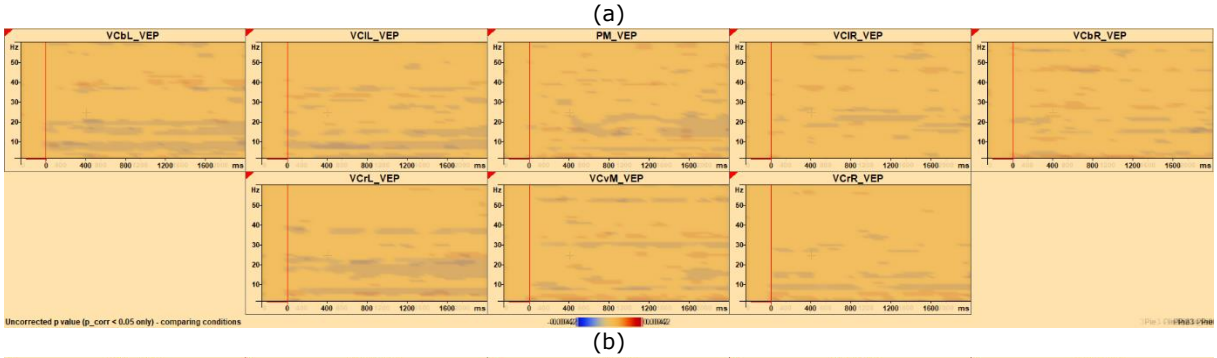

(b)

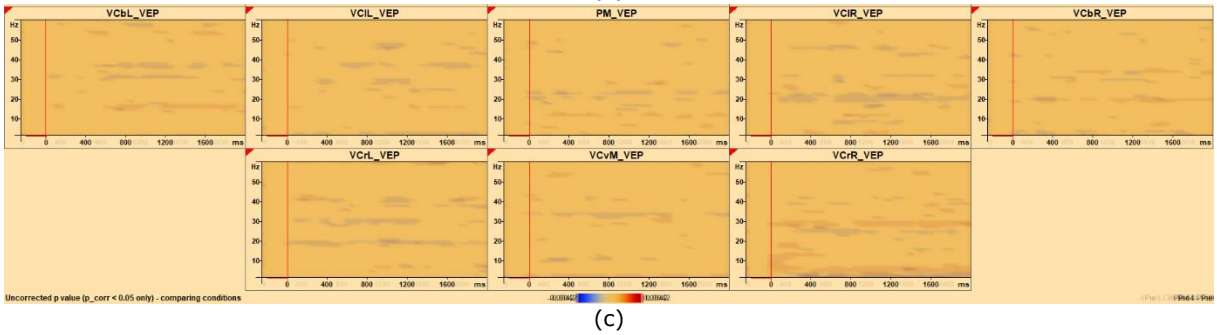

(c)

Figure 3.5 Composite Image target-vs-control: TSE Probability Map (a) Pie2-Pie0, (b) Pie3-Pie0, (c) Pie4-Pie0. These images were generated by averaging the pixel values of the 12 participants' overlaid images. None of the channels show noticeable average brain activity. This suggests the presence of individual variation across participants.

[14] A positive side effect of using a *target vs control* condition was that the rhythmic artifacts were removed and distortions due to filtering got compensated.

3.2 Individual based analysis – a fresh approach

Two participants were shortlisted for analysis on an individual level. The criterion for selection of participant was based on the number of noisy EEG channels. Participant O's data had one interpolated channel with 95.6% accepted trials after the artifact rejection in BESA. Participant T's data had 1 bad channel, and 2 interpolated channels with 88.9% accepted trials (refer table 3.2 for exact number of trials).

Table 3.2 Parameters in individual analysis

Case	Condition	Ecological Variable (Hz)	Good Trials (total 30)	Source Channel	Frequency Band (Hz)	FFT Component (Hz)	FFT Amplitude
O_a	Pie2	0.53316	29	VCrL	32.5	1.3157	0.1312
2.5Hz 20ms	Pie3	0.799753	29	VCrL	32.5	2.1929	0.1057
	Pie4	1.06633	28	VCrL	32.5	1.3157, 2.6315	0.0982, 0.1061
O		*Interpolated Channels*: 1				*Bad Channels*: 0	
T_c	Pie2	0.53316	28	VClR	32.5	3.0701	0.0773
2.5Hz 20ms	Pie3	0.799753	24	VClR	32.5	4.8245	0.0667
	Pie4	1.06633	28	VClR	32.5	3.0701, 7.4561	0.0520, 0.0477
T		*Interpolated Channels*: 1				*Bad Channels:* 2	

3.2.1 Participant O

TSE plots were calculated at a resolution of 2.5Hz 20ms for frequency range of 5Hz – 50Hz. After artifact rejection, 29 trials for Pie2-Pie0, 29 trials for Pie3-Pie0, 28 trials for Pie4-Pie0 conditions were accepted. *VCrl* source channel was selected to find a narrow frequency band of interest based on TSE probability maps (figure 3.6 (d)). After visual inspection, 32.5Hz band of TSE was selected for further analysis (figure 3.7). Magnitude of spectrum was calculated for the 32.5Hz band using FFT (figure 3.8 (b)). Distinct components with the highest amplitudes were noted across three conditions (black stars in figure 3.7 (b)). Pie2-Pie0 showed distinct peak from other conditions at 1.3157Hz with an amplitude of 0.1312 3. Pie3-Pie0 showed distinct peak at 2.1929Hz with an amplitude of 0.1057. Pie4-Pie0 showed distinct peak at 2.6315Hz with an amplitude of 0.1061. Pie4-Pie0 also had another amplitude peak at 1.3157Hz with amplitude 0.0982, which had the same frequency component as Pie2-Pie0 FFT peak.

To check whether a different resolution of TSE with higher time samples, also show distinct FFTs, the same analysis as in the previous paragraph was conducted for 5Hz 10ms resolution. All other conditions were kept unchanged. The results did not show distinct peaks at this resolution. All the peaks for 3 different target vs control conditions occurred at same frequency (1.3Hz) in spectral magnitude (Refer appendix 2c for more details).

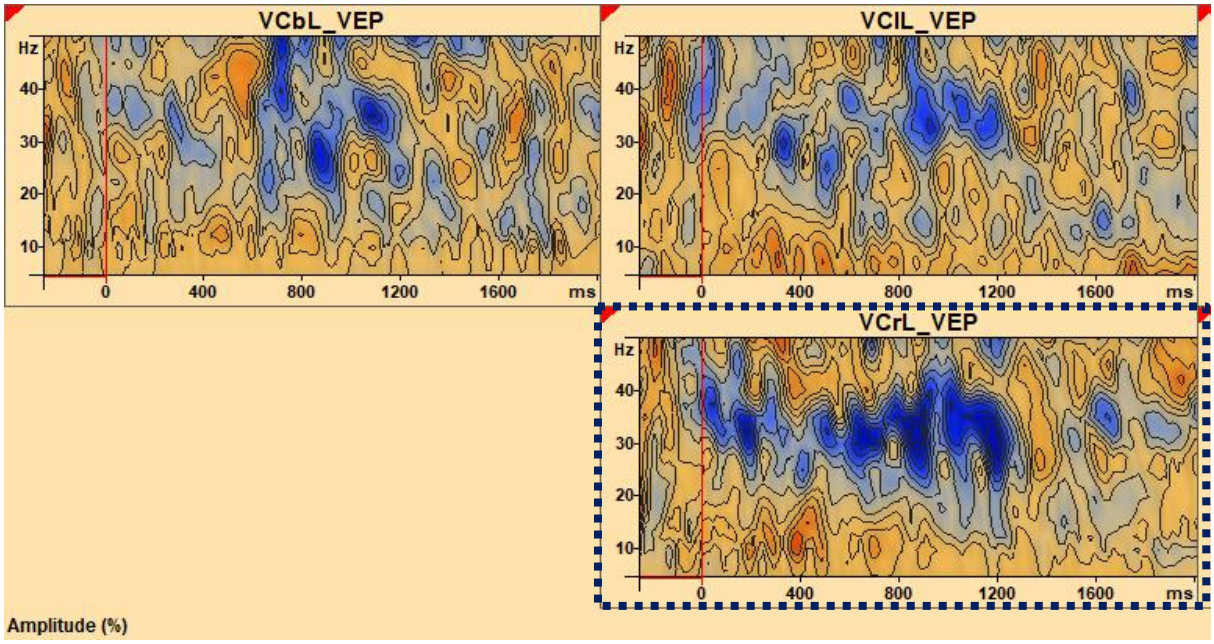
VCbL_VEP
VCIL_VEP
VCrL_VEP
Hz
40
30
20
10
0
400
800
1200
1600
ms
Amplitude (%)

(a)

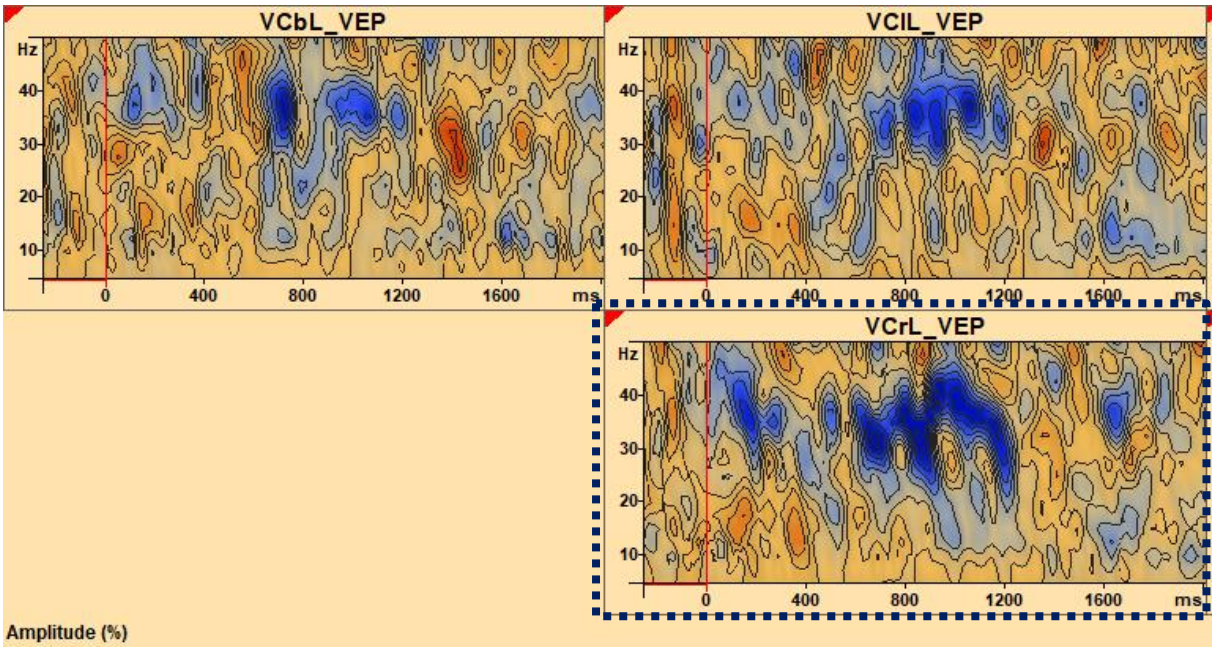
VCbL_VEP
VCIL_VEP
VCrL_VEP
Hz
40
30
20
10
0
400
800
1200
1600
ms
Amplitude (%)

(b)

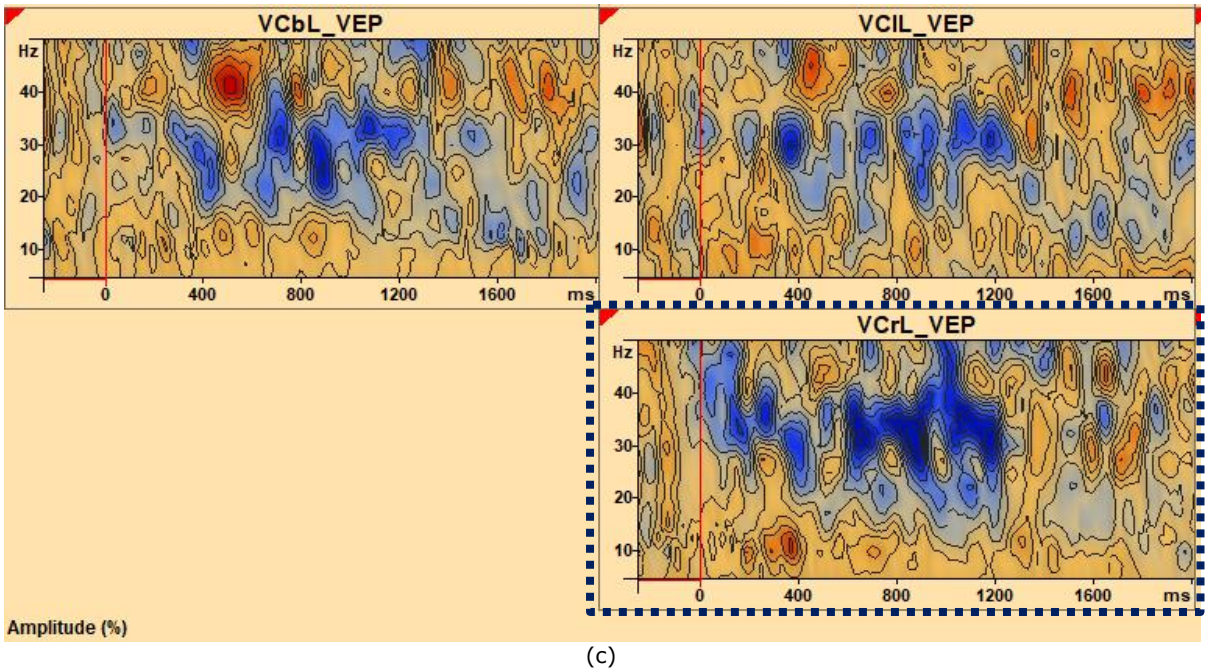

(c)

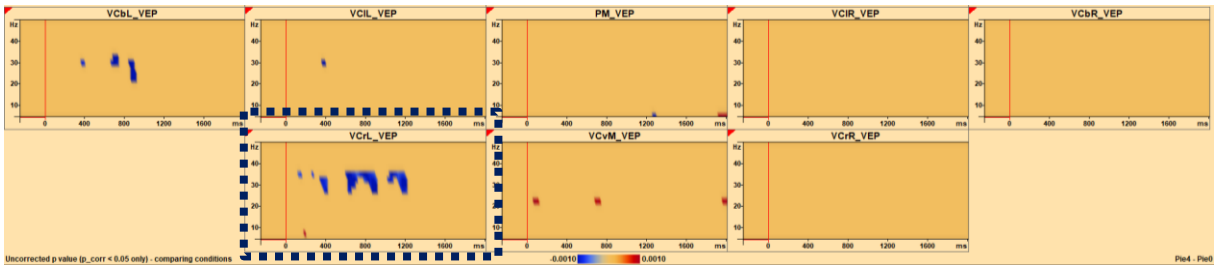

(d)

Figure 3.6 Case O_a TSE Plots (a) Pie2-Pie0 (b) Pie3-Pie0 (c) Pie4-Pie0 (d) Probability Map: Pie4-Pie0. Dotted rectangle shows the source channel of interest – VCrL (Visual Cortex radial Left), y axis is frequency in Hertz, and x axis is time in millisecond. ERD is in blue, and ERS is in red. (a), (b), and (c) show contour map at 63% scale. (d) shows significant ($p<0.05$) ERD or ERS. In (d) sustained significant ERD activity is found in VCrL channel.

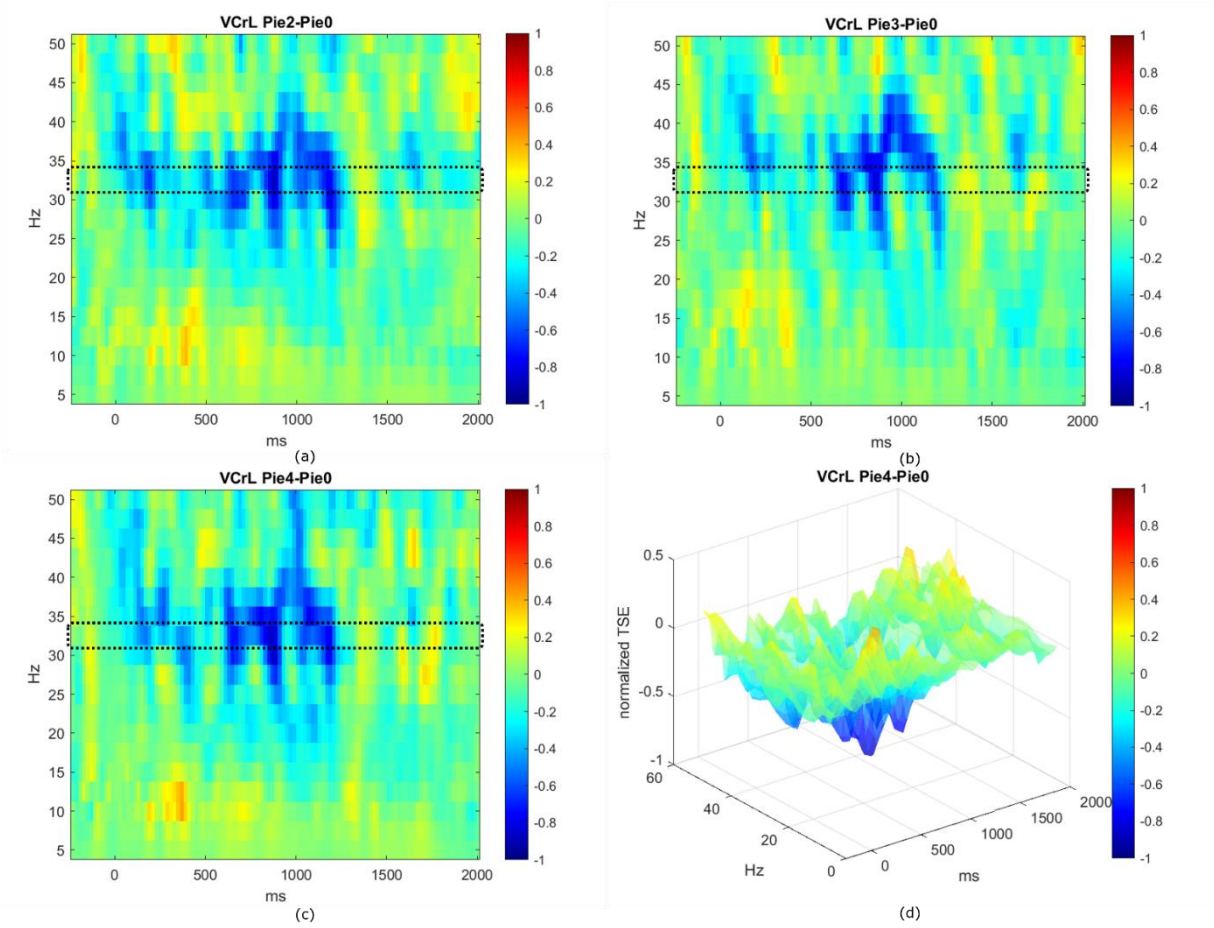

Figure 3.7 Case O_a VCrL Pixel Plot (a) Pie2-Pie0 (b) Pie3-Pie0 (c) Pie4-Pie0 (d) 3D plot Pie4-Pie0. For (a), (b), (c) x axis represents time in milliseconds, and y axis represents frequency bands in Hertz. Normalized TSE has been plotted as per the colour bar on the right of each diagram. 32.5Hz band was selected based on the indication from TSE probability maps for each condition (figure 3.6 (d)) and sustained high ERD across a longer time duration.

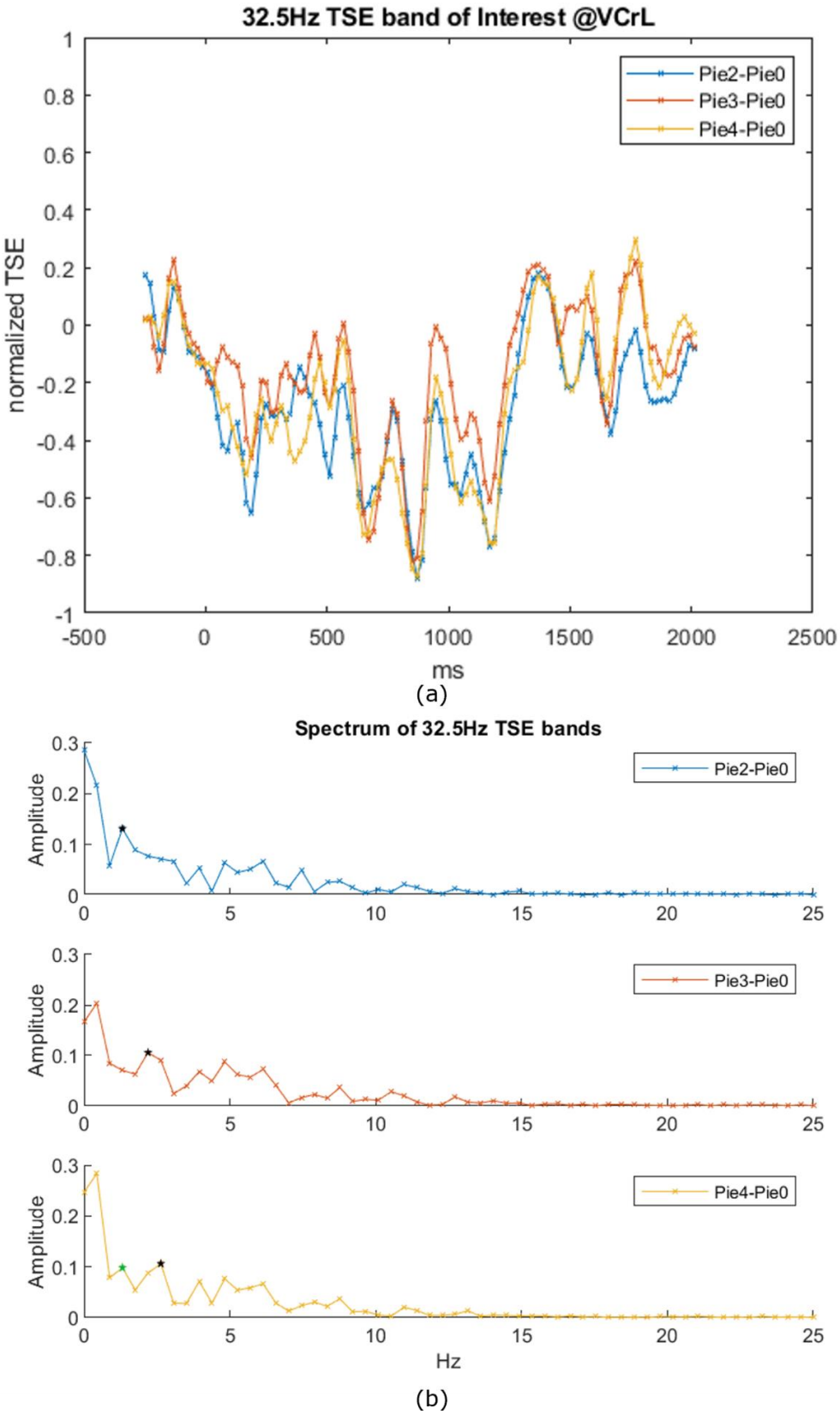

Figure 3.8 Case O_a Extraction of FFT Components (a) ERD bands of interest for 3 conditions (b) Magnitude of spectrum for each ERD band of interest. In (a) 32.5Hz band from TSE data was plotted for all three conditions in a single plot with respect to time. In (b) FFT components were plotted for each condition's 32.5Hz band. Black stars (★) represent the distinct frequency components with highest peak values for respective condition. (Refer table 3.2 for values) Green star (★) represents a second peak in Pie4-Pie0 condition with the same FFT component as that of Pie2-Pie0.

3.2.2 Participant T

TSE plots were calculated at a resolution of 2.5Hz 20ms for frequency range of 5Hz – 50Hz. After artifact rejection, 28 trials for Pie2-Pie0, 24 trials for Pie3-Pie0, 28 trials for Pie4-Pie0 conditions were accepted. For this participant's data the probability maps did not show any significant value in the visual cortex source channels (figure 3.9 (d)). So a hit a trial process had to be used. The highest ERD was found in VCbL, around 22.5Hz and 25Hz. Therefore, these bands were extracted and their FFT was calculated. For both frequency bands 22.5Hz and 25Hz, Pie2-Pie0 (3.0701, 3.0701) and Pie4-Pie0 (6.1403Hz, 5.7017Hz) followed the trend, where Pie4-Pie0 had a distinct spectral peak component greater than Pie2-Pie0. Pie4-Pie0 also had another peak at the same frequency component as Pie2-Pie0 (3.0701Hz). Pie3-Pie0 (1.3157Hz, 0.4385Hz) did not follow the trend and gave a peak at lower frequencies than both Pie2-Pie0 and Pie4-Pie0. (See appendix 2e, 2f and 2g for figures and table of values)

For the third attempt, *VClR* source channel was selected to find a narrow frequency band of interest based on relatively high ERD that sustained for a longer duration of stimulus period. After visual inspection, 32.5Hz band of TSE was selected for further analysis (figure 3.10). Magnitude of spectrum was calculated for the 32.5Hz band using FFT (figure 3.11 (b)). Distinct components with the highest amplitudes were noted across three conditions (black stars in figure 3.11 (b)). Pie2-Pie0 showed distinct peak from other conditions at 3.0701Hz with an amplitude of 0.0773. Pie3-Pie0 showed distinct peak at 4.8245Hz with an amplitude of 0.0667. Pie4-Pie0 showed distinct peak at 7.4561Hz with an amplitude of 0.0477. Pie4-Pie0 also had another amplitude peak at 3.0701Hz with amplitude 0.0520, which had the same frequency component as Pie2-Pie0 FFT peak.

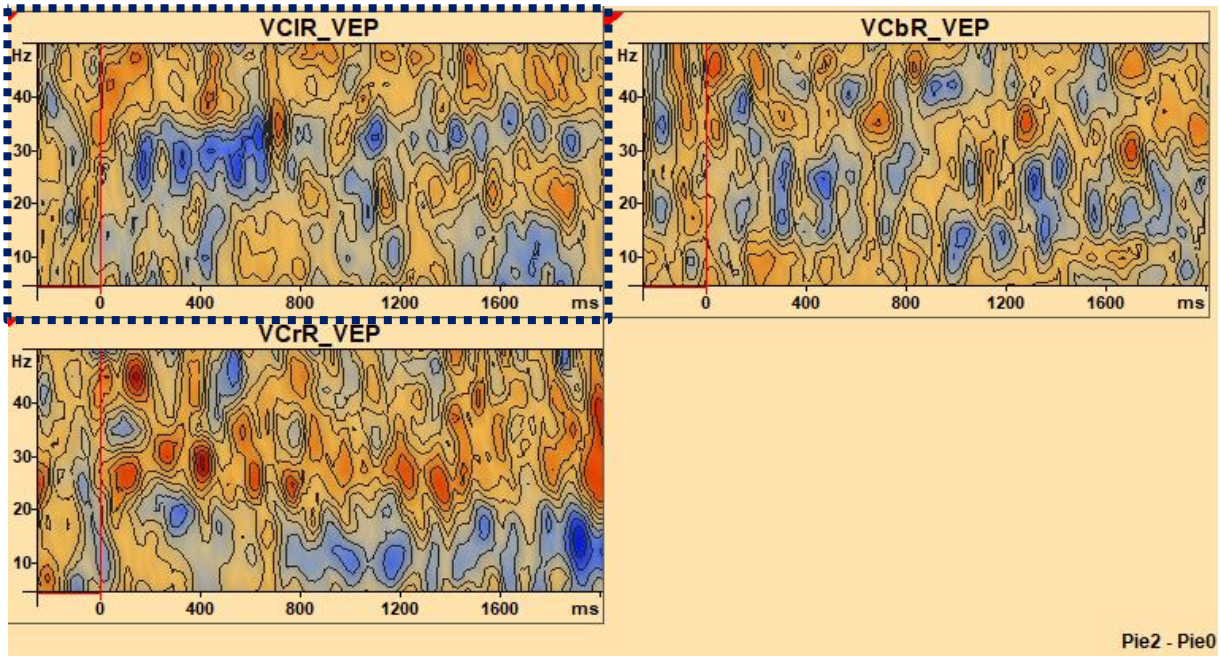

(a)

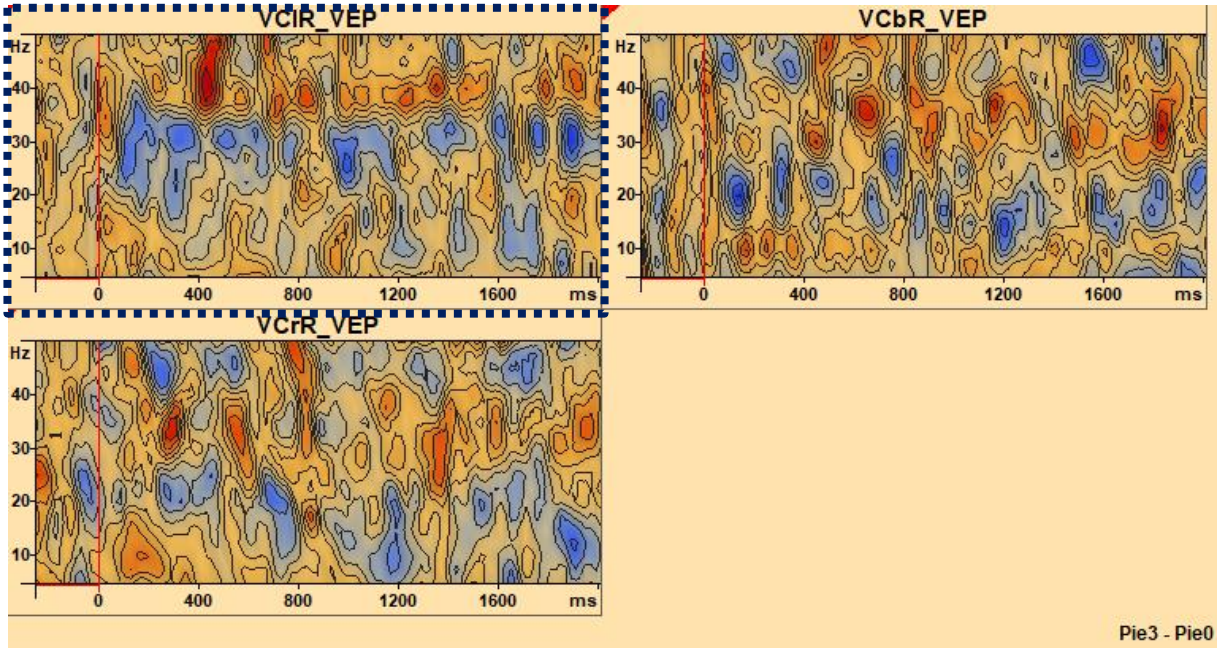

(b)

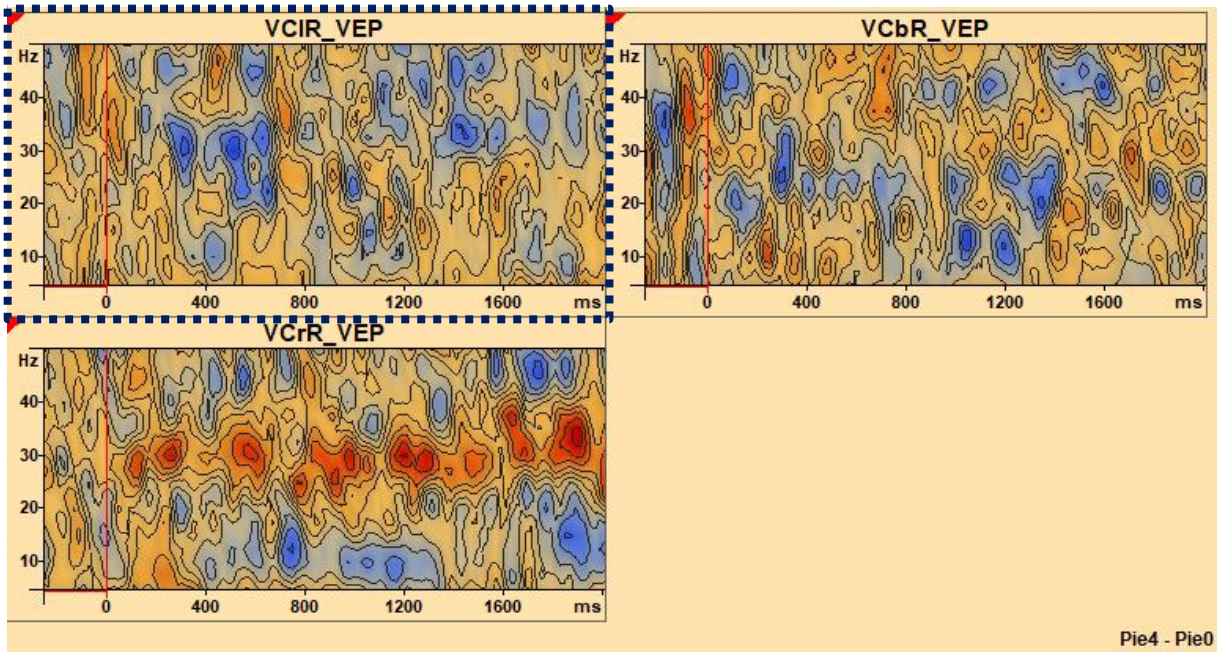

(c)

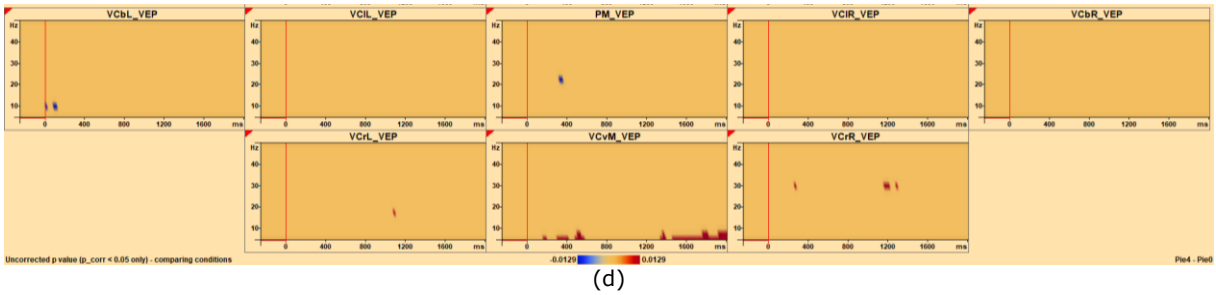

(d)

Figure 3.9 Case T_c TSE Plots (a) Pie2-Pie0 (b) Pie3-Pie0 (c) Pie4-Pie0 (d) Probability Map: Pie4-Pie0. Dotted rectangle shows the source channel of interest – VCIR (Visual Cortex lateral Right), y axis is frequency in Hertz, and x axis is time in millisecond. ERD is in blue, and ERS is in red. (a), (b), and (c) show contour map at 63% scale. (d) shows significant ($p<0.05$) ERD or ERS. Note that (d) does not show sustained significant ERDs in the Visual Cortex source channels.

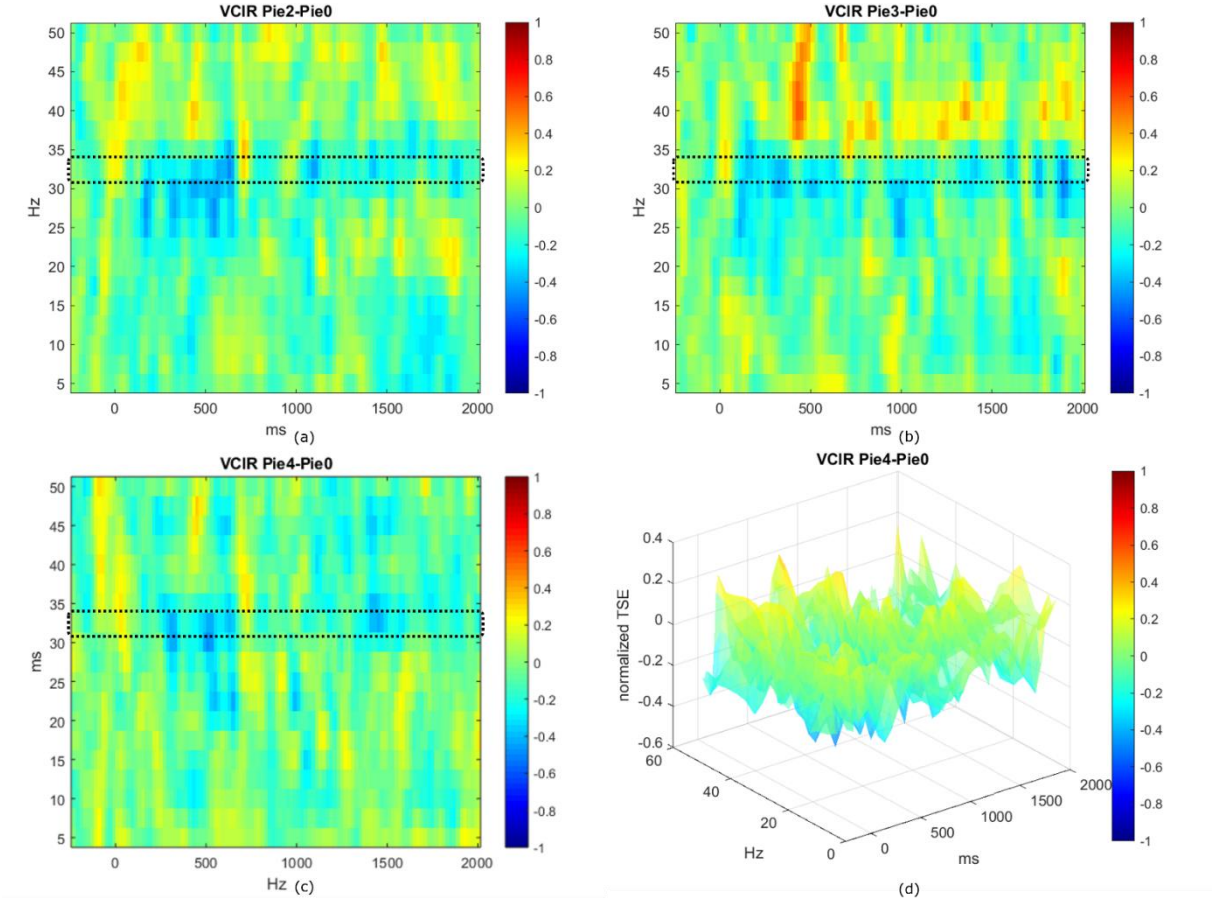

Figure 3.10 Case T_c VCIR Pixel Plot (a) Pie2-Pie0 (b) Pie3-Pie0 (c) Pie4-Pie0 (d) 3D plot Pie4-Pie0. Normalized TSE has been plotted as per the colour bar on the right of each diagram. 32.5Hz band was selected based on the indication from TSE probability maps for each condition (figure 3.6 (d)) and sustained high ERD across a longer time duration.

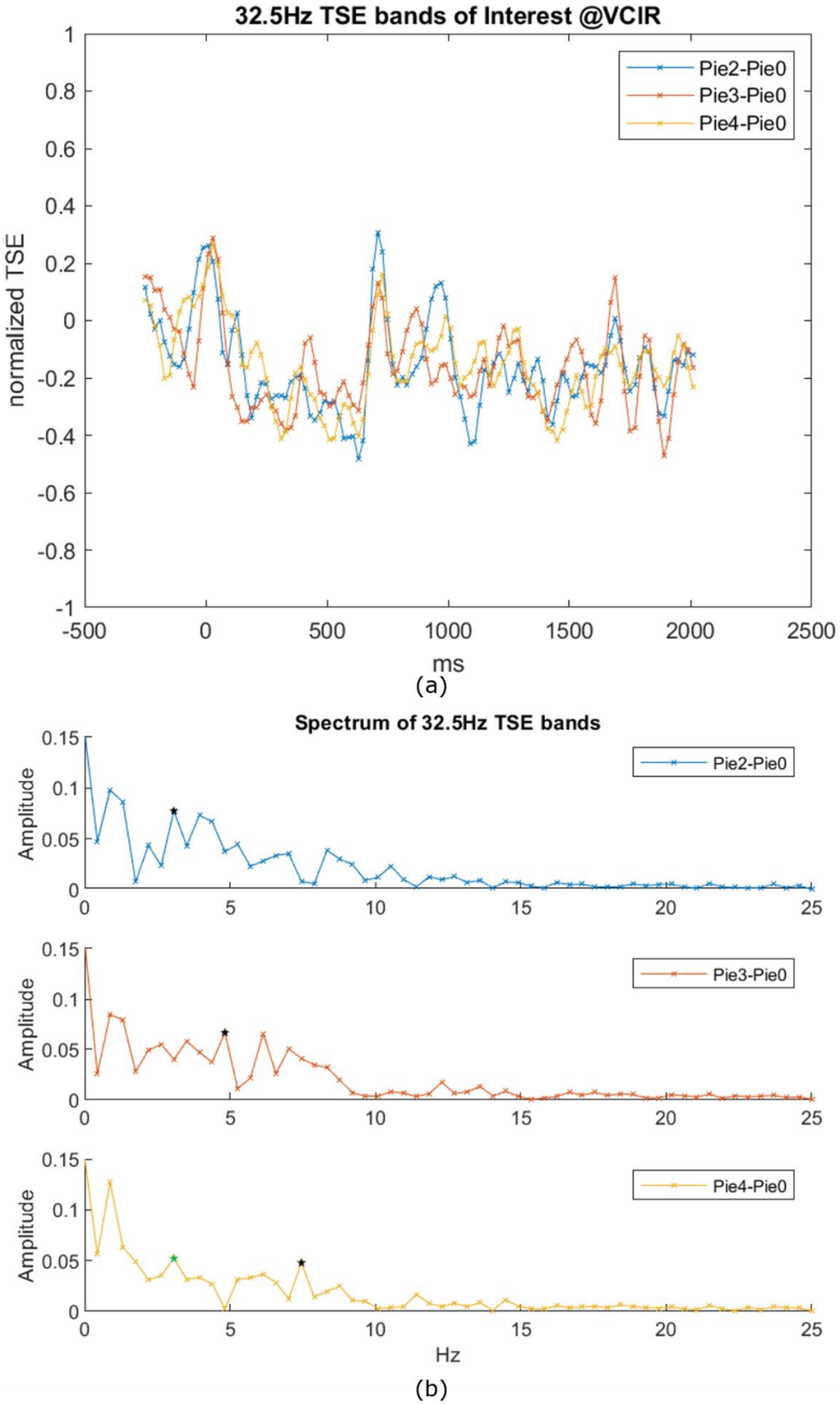

Figure 3.11 Case T_c Extraction of FFT Components (a) ERD bands of interest for 3 conditions (b) Magnitude of spectrum for each ERD band of interest. In (a) 32.5Hz band from TSE data was plotted for all three conditions in a single plot with respect to time. In (b) FFT components were plotted for each condition's 32.5Hz band. Black stars (★) represent the distinct frequency components with highest peak values for respective condition. (Refer table 3.2 for values) Green star (★) represents a second peak in Pie4-Pie0 condition with the same FFT component as that of Pie2-Pie0.

3.3 Ecological vs Neural Scale

After obtaining the values in table 3.2, MATLAB's curve fitting toolbox was used to arrive at the following linear relationships. Linear model is based on the equation: f(x) = p1*x + p2. p1 is the slope for the linear equation, and also the coupling parameter '*k*'. FFT components obtained from TSE bands of interest is N_D (neural dynamics) and f(x) in the linear equation. Ecological variable is the perceptual information ψ, and x in the equation. If we rewrite the equation as f(x) = p1*(x + p2/p1), then $N_D = k(\psi + c)$, where c is a constant p2/p1.

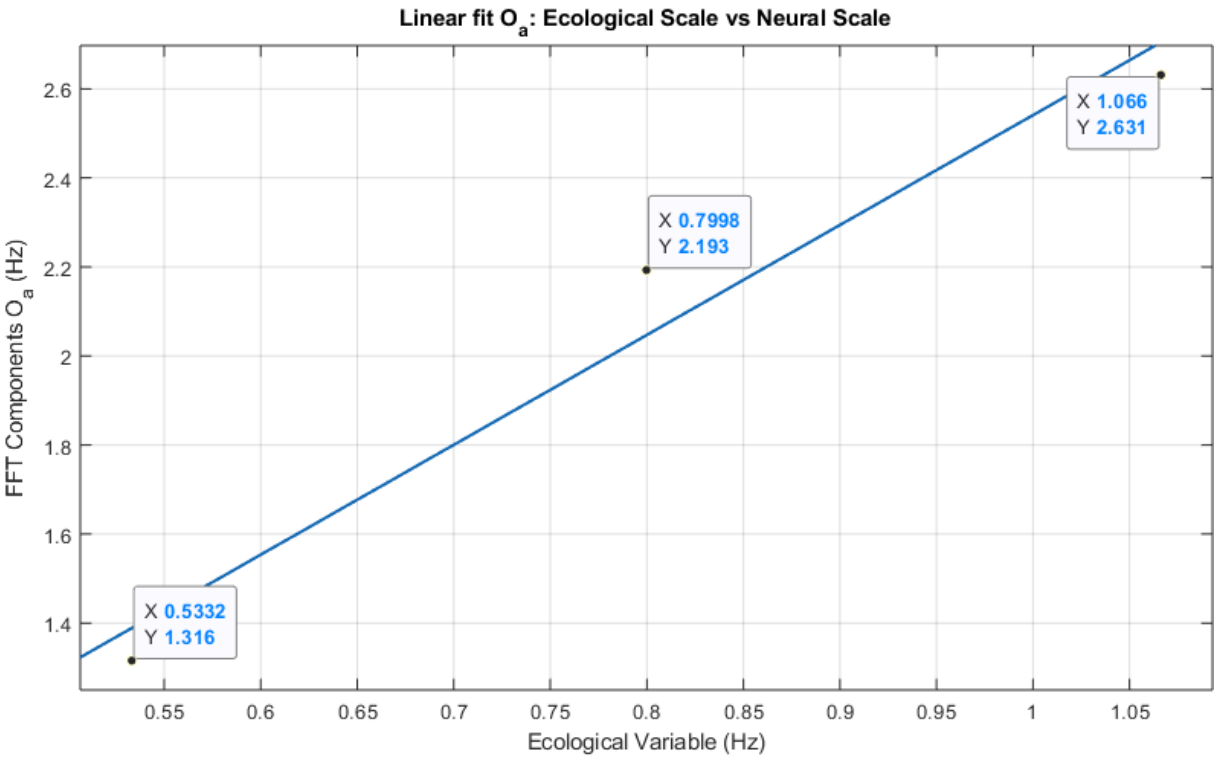

Figure 3.12 Linear coupling relationship for Participant O The figure above shows the best fit line in blue and the actual data plotted in black dots. Values are picked from table 3.2. Y axis represents the frequency components of distinct peaks, and X axis represents the ecological scale.

For participant O, coefficients (with 95% confidence bounds) of the linear equation are, p1 = 2.468 (-3.566, 8.502) and p2 = 0.07301 (-4.928, 5.074). p1 is the slope of the line in the figure 3.12, and the coupling parameter 'k'. Goodness of fit statistics are, SSE: 0.03206, R-square: 0.9643, Adjusted R-square: 0.9286, and RMSE: 0.179.

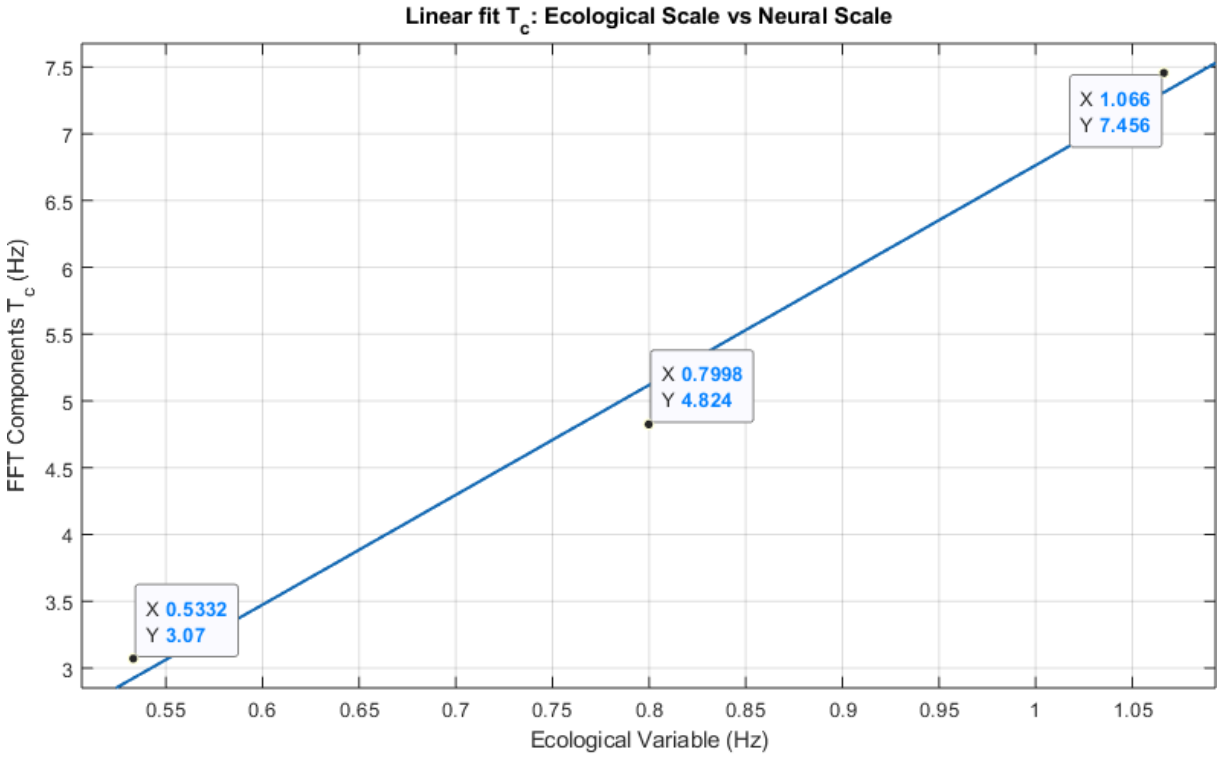

Figure 3.13 Linear coupling relationship for Participant T The figure above shows the best fit line in blue and the actual data plotted in black dots. Values are picked from table 3.2. Y axis represents the frequency components of distinct peaks, and X axis represents the ecological scale.

For participant T, coefficients (with 95% confidence bounds) are p1 = 8.226 (-3.845, 20.3) p2 = -1.462 (-11.47, 8.543). p1 is the slope of the line in the figure 3.13, and the coupling parameter 'k'. Goodness of fit statistics are, SSE: 0.1283, R-square: 0.9868, Adjusted R-square: 0.9737, and RMSE: 0.3582.

4 Discussion

We will first We will first discuss the direct implications of the results. After that, we can discuss the practical and far-reaching consequences of our results. In the end we conclude our study.

4.1 Stimulus design and Ecological validity

Broderick et al. (2022) makes use of pinwheel sinusoidal gratings in a fMRI study. Gallant et al. (1993) has used pinwheel gratings to study the response of V4 area in visual cortex in macaque monkeys. Kleinschmidt et al. (2002) comes to closest to our stimuli. They studied object rotation using pinwheel stimulus (calling it a windmill pattern) made from a real disc with 12 alternating black and white circular sectors (our study used 2,3 and 4 sectors) in a fMRI study. They compared stationery and motion conditions. Wagon wheel illusion uses high rotations per minute (Purves et al., 1996). To our best knowledge the stimuli used in this study are novel.

There is strong evidence for looming related ERPs in visual motion perception studies for infants (van der Weel, van der Meer, 2009). We aspired to come up with a stimulus that has high ecological validity. Therefore, this study combines looming and rotation, while using looming template from the same study.

This lab-based stimuli are a recreation of several real-world situations. For instance, a person could accelerate in a car or a train looking at a windmill. Another example is where a cricketer or a baseballer stands to catch the ball or where the batter is waiting to hit a ball. Quite often, the ball is spinning distinguished by the U-shaped seam of the baseball ball or the single seam of a cricket ball.

4.2 Perceptual Information at the Ecological Scale

To answer what is the perceptual information in the stimulus, one needs to disassemble the stimuli. The stimuli are animated 2D projections of 3D virtual objects. These animations are 60 different pictures or frames (60Hz screen refresh rate). For each picture it is possible to calculate spatial frequency in 2 dimensions – x and y dimension. Each frame succeeds the previous as per the rotation and looming relationships explained in section 2.1.2. One has two choices here, either calculate the successive spatial frequency plots for all 60 frames/sec for the entire duration of the trial or use the trajectory equations in 2.1 (ii), (iii) to calculate frequency transforms for x coordinate and separately for y coordinate.[15]

However, both approaches implicitly incorporate simultaneous rotation and looming. This poses a problem, as looming stimuli have been shown in research (van der Weel, van der Meer, 2009) to be tau-coupled with the first order derivative of the averaged source waveform (for babies). Tau is a ratio-based relationship (Lee, 2009), between the action gap and the rate of closure of action gap. So, there is a precedence to look at other visual motion phenomenon, which might help establish relationship between/tie some

[15] There is also a third approach, that combines the spatial frequency, and frequency transforms of x and y coordinate. In appendix 3a, the figure shows the spatial frequency of the trajectory figure.

frequency-based parameter in the stimuli, to the time-frequency domain analysis of EEG data.

As TSE analysis allows comparison of target vs control, we created a control condition with pure looming (catch trial), that would remove the effects of looming from the target conditions. Which means, rotation related physical parameter used to quantify perceptual information in the stimulus. With the caveat, that the rotational parameter is operating in an optic flow paradigm.

4.3 Implications of Averaging Analysis

All the single experimental conditions of interest with substantial significant values in the probability maps, show desynchronization. Even the catch trial, which does not have any pattern, and hence does pure looming (no rotation), shows desynchronization (in section 3.1.1). Based on literature about time-frequency analysis in visual motion perception, one might argue that ERD in upper alpha band signifies active cognitive engagement in a participant (Pfurtscheller et. al 1994). However, Pfurtscheller et. al (1994) do not comment about beta band and gamma band desynchronization.

The similarity in frequency bands, 8Hz band in VCrL and VClL might signify oscillatory activity for similar aspects of visual motion perception across the four different experimental conditions. In VCrR, 12Hz frequency is the common band with ERD across all four conditions, suggesting the engagement of neuronal assemblies for similar functions. What could these similar activities be? One could argue that visual perception with regards to looming related responses would be the most likely suspect of these shared frequency band ERDs. If that is the case, then what does it mean for the remaining frequency bands with ERD? Does it mean that these are the responses to differentiating aspects of the stimuli? Unfortunately, the observed data does not reveal trends suitable to comment on the last question.

In VCrL, on a superficial level the lowerbound frequency might suggest the oscillatory activity corresponding to the differences in the 3 target conditions. If one builds up on this line of reasoning, then Pie3, is the odd one out of the 4 conditions. Pie2 and Pie4 have the same upperbound frequency band of 12Hz. Moreover, Pie4's ERD bands (8 – 12Hz) are a subset of Pie2's bands, with 4Hz band having regular ERD bursts after 200ms. This could imply Pie4 shares a high overlap with Pie2, with a distinguishing component.

In VCrR too, Pie4 shares a high overlap with Pie2, with a distinguishing component. Could Pie2 be a special case of Pie4?[16] We will revisit this question in the next section. This analysis reveals that Pie0 has similarity with Pie2, Pie3, and Pie4. To find evidence for ecological resonance, it would be one's prime imperative to find evidence that helps in distinguishing the target conditions. Only when there is no ambiguity in the evidence to differentiate the three target conditions, it would be prudent to proceed with further analysis to find the link between the ecological and the neural scale. Analysis of probability map composites of single experimental conditions did not reveal evidence to support our hypothesis.

The lack of our ability to comment on the distinction between the three conditions based on single condition TSE probability maps, led us to check the target vs control condition

[16] We find more evidence for shared characteristics between Pie4-Pie0 and Pie2-Pie0 condition in section 3.2.

TSE probability maps. These, however, do not show any trends whatsoever to allow any inference. This null result is albeit an indicator of variations at the individual level.

Choosing 2 participants with relatively clean (artifact free) data, allows one to analyse without bothering about data fidelity in case of a novel exploratory study.

4.4 Implications of the individual-based analysis

Guided by the lack of trends across participants for target vs control conditions, we move onto a new type of analysis that gauges TSE plots (not the probability maps) for individual participants. The comparison of control condition (catch trial, Pie0 – without any pinwheel pattern) vs the target conditions (Pie2, Pie3, Pie4 with pinwheel patterns), mathematically subtracts the TSE values of Pie0 from Pie2, Pie3, and Pie4 respectively, to give three conditions – Pie2-Pie0, Pie3-Pie0, and Pie4-Pie0.

What does this mathematical subtraction or comparison of condition essentially mean? The catch trial is a pure looming case, with no rotation. By deductive reasoning, subtracting the perceptual brain responses (EEG TSE) from a case with rotation + looming, would only leave rotation. In other words, target conditions have both rotation and looming motion dynamics in them, whereas control condition has only looming motion dynamics. When compared, target vs control would contain only the perceptual components (brain responses) related to the rotational motion dynamics. This is where one needs to think carefully, this rotation is not context independent rotation. *It is a rotation within optic flow paradigm.* It is most certainly different from a purely rotating stimuli at a stationary distance.[17]

Moreover, the baseline is itself a rotating object at a stationary distance. TSE is a measure normalized with baseline. This helps to ensure that we the TSE components are not a continuation of the baseline activity.

With the understanding of what we are measuring (rotation in optic flow), we can now dismantle the analysis. For the O_a case, probability maps without regression gave the best indication of the ERD of interest, i.e. in the VCrL source channel. Regression before calculating the probability maps, worsened the detection. The probability maps had lesser ERD activity after regression was applied. This is correct in principle, as regression is supposed to separate the evoked activity from the induced activity. However, for T_c case, the probability maps didn't yield significant values for any of the source channels. Regression before probability calculation yielded some significant components in theta band activity (both ERD and ERS), however, that does not correspond to the gamma band ERD in O_a case. Moreover, one would look for large ERD activity across all three conditions in the same source channel. The probability maps after regression, do not provide any single channel that has ERD across all three conditions.

This begs the question, if regression is a good tool after all for a visual motion experiment? The evoked activity is defined as the brain activity bound to stimulus, and the induced activity is the brain activity that follows later (as a result of induction of the surrounding areas by the evoked brain area). In a visual motion study, especially like the

[17] Why did we use the looming paradigm? Doesn't it complicate things? In real life, it's more likely to see ecologically rich stimulus. The science should adapt to real life, and we should come up with techniques and tools to unravel the fabric of reality (deepen our understanding), rather than distort or adapt real life events to the point, where it becomes easier for us to do science.

current one, where neither the baseline period has stationary object, nor the stimulus period has a stationary object, and the transition between baseline to stimulus period is seamless, one can argue that evoked and induced can't be held to apply in the traditional sense.

Absence of significant values in the probability maps for participant T, led to a bit of trial and error. Appendix 2e shows the first 2 failed attempts to detect an increasing trend for the FFT components. In both calculations, Pie3 does not lie on the trend. The third attempt (in section 3.2.2) shows the trend that supports our hypothesis.

In both cases, ERDs at 32.5Hz contain the FFT components that provide evidence to support our hypothesis. It may or may not suggest that 32.5Hz is the specific band across all people to handle rotation in optic flow. We will need to analyse more participants, to observe any emerging trend and do statistical analyses. O_a has supporting evidence for ecological resonance in the left hemisphere, whereas T_c has it in the right hemisphere. The only difference between them is that T is an avid gamer. The different coupling parameter values could perhaps be further explored to carry out brain fingerprinting using EEG, if coupling parameters are unique and repeat for a person across sessions (Finn et al., 2015).

Can we draw some generalizations about detecting ERD patterns based on our 2 results that might provide supporting evidence for ecological resonance? Based on case O_a, it might seem that highest ERD across all channels should be given preference. However, that doesn't hold true for T_c. Based on case T_c, it makes sense to look for ERD that is spread the most across the entire stimulus period, meaning that, that specific frequency band (with widespread ERD) is the cognitively engaged throughout the stimulus period. This should also persist across all three conditions (Pie2-Pie0, Pie3-Pie0, and Pie4-Pie0) for an individual participant. These two points hold true for O_a as well. So, a rule of thumb can be suggested based on these observations. One should look for channels where ERDs persist across a narrow frequency band for a large duration of stimulus period, and these ERDs should also show across the three TSE comparison conditions.

Coming over to this new measure of FFT component, what does it mean to calculate the FFT component of a frequency band of TSE?

Qualitatively, an ecological variable constrains (or drives) the neural dynamics. Neural dynamics can be any variation of the brain response. In our case it is the frequency component (FFT) of the ERD band of interest in a specific source channel.

When neuronal assemblies are recruited, they can spike but need a refractory period (refill) afterwards until they become active again. It is this time when another nearby neuronal assembly might substitute for the earlier neurons now in their refractory period. The call for a minimum collection of neuronal assembly is on as long as the stimulus lasts, creating a cyclical operation. So, in the very next moment, there might be a temporary surge and for sure a relative surge in recruitment resulting in the peak of the ERD band. This happens again and again - hence we see a sustained oscillation in a specific band inside Temporal-Spectral Evolution (TSE). This cyclical operation sits well with Anderson's neural reuse theory (Anderson, 2010).

This would mean that the FFT peaks (from ERD frequency bands) are resonant frequencies, qualitatively and quantitatively!

Why do we see common frequency components with higher amplitudes in FFT plots? A possible reason could be that the common frequency components represent the common class of perception for these spinning objects or some lower visual motion processing components or both. The first distinct FFT components in respective target vs control conditions, are the distinguishing components because of the difference in pinwheel patterns.

Complex demodulation comes with a trade-off between time and frequency resolution. Higher the time resolution, greater the frequency spread in FFT's magnitude spectrum calculation. However, with higher time resolution, we get a lower frequency resolution, which might mask the ERDs that could help unlock the linear relationship. The graphs in appendix 2d and 2e show that no meaningful distinction arises if the resolution 5Hz, 10ms is used.

Conclusion

Ecological resonance is proposed to be a cognitive architecture that is capable of mathematically and qualitatively explaining the relationship between the ecological and the neural scale in ecological psychology. To find biological evidence we conducted a visual motion perception study by designing a novel stimulus with high density EEG on adults. We adopted the proposition by the theory of ecological resonance that there should be a coupling relationship between perceptual information and neural dynamics, as our hypothesis. We found evidence of a linear relationship between the frequency or return to orientation (at the ecological scale) and FFT of the TSE band (at the neural scale) for 2 participants. This result strongly supports ecological resonance. We also discuss the biological implications of this new FFT measure and propose how it could mean that neuronal assemblies cycle through multiple subunits to sustain ERD in response to an ongoing stimulus.

References

Anderson, M. L. (2014). *After phrenology: Neural reuse and the interactive brain*. Cambridge, MA: MIT Press

Berg, P., & Scherg, M. (1994). A fast method for forward computation of multiple-shell spherical head models. *Electroencephalography and Clinical Neurophysiology*, 90(1), 58–64. https://doi.org/10.1016/0013-4694(94)90113-9

Broderick, W. F., Simoncelli, E. P., & Winawer, J. (2022). Mapping spatial frequency preferences across human primary visual cortex. *Journal of Vision*, 22(4) doi:10.1167/jov.22.4.3

Chomsky, N. (1980). *Rules and representations*. Oxford, UK: Basil Blackwell.

Davidson, A.C. and Hinkley, *D. V.: Bootstrap Methods and their Application, Chapter 4.4.1: Studentized bootstrap method*. Cambridge University Press, 1999

Ferree, T. C., Luu, P., Russell, G. S., & Tucker, D. M. (2001). Scalp electrode impedance, infection risk, and EEG data quality. *Clinical Neurophysiology, 112*(3), 536–544. https://doi.org/10.1016/S1388-2457(00)00533-2

Finn, E. S., Shen, X., Scheinost, D., Rosenberg, M. D., Huang, J., Chun, M. M., . . . Constable, R. T. (2015). Functional connectome fingerprinting: Identifying individuals using patterns of brain connectivity. *Nature Neuroscience*, 18(11), 1664-1671. doi:10.1038/nn.4135

Frigo, M., & Johnson, S. G. (1998). FFTW: An adaptive software architecture for the FFT. Paper presented at the ICASSP, IEEE International Conference on Acoustics, Speech and Signal Processing - Proceedings, , 3 1381-1384. doi:10.1109/ICASSP.1998.681704

Gallant, J. L., Braun, J., & Van Essen, D. C. (1993). Selectivity for polar, hyperbolic, and cartesian gratings in macaque visual cortex. Science, 259(5091), 100-103. doi:10.1126/science.8418487

Granger, C. W. T. and Hatanaka, M. (1964). *Spectral Analysis of Economic Time Series*. Princeton University Press, Princeton

Gibson, J. J. (1966). *The Senses considered as perceptual systems*. Boston, MA: Houghton Miffin

Gibson, J. J. (1979). *The ecological approach to visual perception.* Boston, MA: Houghton Miffin

Ille, N., Berg, P., & Scherg, M. (2002). Artifact correction of the on-going EEG using spatial filters based on artifact and brain signal topographies. *Journal of Clinical Neurophysiology, 19*(2), 113–124. https://doi.org/10.1097/00004691-200203000-00002

Kleinschmidt, A., Thilo, K. V., Büchel, C., Gresty, M. A., Bronstein, A. M., & Frackowiak, R. S. J. (2002). Neural correlates of visual-motion perception as object- or self-motion. *NeuroImage, 16*(4), 873-882. doi:10.1006/nimg.2002.1181

Lee, D. N. (2009). General tau theory: evolution to date. Perception, 38(6):837–850

Perrin, F., Pernier, J., Bertrand, O., & Echallier, J. F. (1989). Spherical splines for scalp potential and current density mapping. *Electroencephalography and Clinical Neurophysiology, 72*(2), 184–187. https://doi.org/10.1016/0013-4694(89)90180-6

Picton, T. W., Bentin, S., Berg, P., Donchin, E., Hillyard, S. A., Johnson, R., ... Rugg, M. D. (2000). Guidelines for using human event-related potentials to study cognition: Recording standards and pub-lication criteria. *Psychophysiology, 37*(2), 127–152. https://doi.org/10.1111/1469-8986.3720127

Pfurtscheller, G., & Lopes Da Silva, F. H. (1999). Event-related EEG/MEG synchronization and desynchronization: Basic principles. Clinical Neurophysiology, 110(11), 1842–1857. https://doi.org/10.1016/S1388-2457(99)00141-8

Pfurtscheller, G., Neuper, C., & Mohl, W. (1994). Event-related desynchronization (ERD) during visual processing. *International Journal of Psychophysiology*, *16*(2–3), 147–153. https://doi.org/10.1016/0167-8760(89)90041-X

Purves, D., Paydarfar, J. A., & Andrews, T. J. (1996). The wagon wheel illusion in movies and reality. *Proceedings of the National Academy of Sciences of the United States of America*, 93(8), 3693-3697. doi:10.1073/pnas.93.8.3693

Raja, V. (2018). A theory of resonance: Towards an ecological cognitive architecture. *Minds and Machines*, 28(1), 29-51. doi:10.1007/s11023-017-9431-8

Scherg, M., Ille, N., Bornfleth, H., Berg, P., 2002. Advanced Tools for Digital EEG Review:: Virtual Source Montages, Whole-head Mapping, Correlation, and Phase Analysis. *Journal of Clinical Neurophysiology 19,* 91–112. https://doi.org/10.1097/00004691-200203000-00001

Tucker, D. M. (1993). Spatial sampling of head electrical fields: The geode-sic sensor net. *Electroencephalography and Clinical Neurophysiology, 87*(3), 154–163. https://doi.org/10.1016/0013-4694(93)90121-B

Van Der Weel, F. R., & Van Der Meer, A. L. H. (2009). Seeing it coming: Infants' brain responses to looming danger. *Naturwissenschaften, 96*(12), 1385-1391. doi:10.1007/s00114-009-0585-y

Image Sources

Institut Pasteur, (2013). research_pasteur-imagehandler.jpg (800×392). [online] research.pasteur.fr. Available at: https://research.pasteur.fr/wp-content/uploads/2017/06/research_pasteur-imagehandler.jpg [Accessed 5 Dec. 2022].

Rest of the images are taken from BESA 7.0, created programmatically in MATLAB, or created by the author.

Appendices

Appendix 1: **Supplementary information for Methods Section**

1a *Video link showing few trials: https://youtu.be/01k8lKk50UI*

1b *Program Flow Structure for the experiment in E-Prime 2.0*

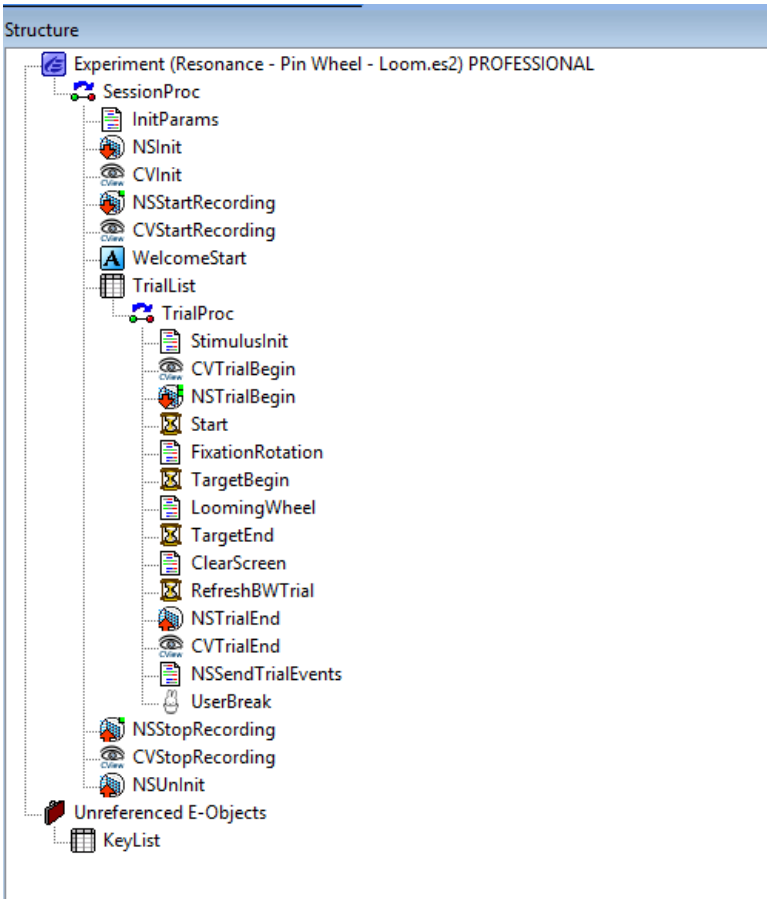

1c *Code to program the experiment in E-Prime 2.0*

```
Function GetDiam(dist As Double) As Double
	Dim diam As Double
	diam = pPerCM * circleDiam * screenDist / dist
	If (diam < 0 And diam > 10000) Then
		diam = 10000
	End If
	GetDiam = diam
End Function
Sub Wheel (pieRadius As Double, pies As Integer, degrees As Double)
	Dim i As Integer 'for loop
```

```
	Dim col As Double
	tempCanvas.FillColor = backgroundColor
	tempCanvas.Clear
	'Trial Counter
	tempCanvas.Text Display.XRes - 45, 0, trialNumber

	'circular outline
	tempCanvas.PenColor = CColor ("00,00,00")
	tempCanvas.PenWidth = pieRadius*8/100
	tempCanvas.Circle Display.Xres/2, Display.Yres/2, pieRadius
	tempCanvas.PenWidth = 1

	If pies = 0 Then
		tempCanvas.FillColor = CColor ("00,00,00")
		tempCanvas.PenColor = CColor("00,00,00")
		tempCanvas.Circle Display.Xres/2, Display.Yres/2, pieRadius

		Else
			For i = 1 To pies

				tempCanvas.FillColor = CColor ("00,00,00")
				tempCanvas.PenColor = CColor("00,00,00")
				tempCanvas.Pie Display.Xres/2, Display.Yres/2, pieRadius, (2*(i-
1)*180/pies) + degrees, ((2*i-1) * 180/pies) + degrees
		'tempCanvas.PenColor = col
		'tempCanvas.FillColor = col'CColor(col & "," & col &"," & col)
				tempCanvas.FillColor = CColor ("255,255,255")
				tempCanvas.PenColor = CColor("255,255,255")
				tempCanvas.Pie Display.Xres/2, Display.Yres/2, pieRadius, ((2*i-
1)*180/pies) + degrees, (2*i*180/pies) + degrees
			Next i
	End If
End Sub
	''''''''''''''''''''''''''''''''''''''''''''''''''''
	' InLine - InitParams BEGIN <InitParams>
	''''''''''''''''''''''''''''''''''''''''''''''''''''
backgroundColor = CColor("220,220,220")
attentionDuration = 250 'duration for fixation-rotation
'1920 x 1080 | width for surface hub = 104.6 cm | length = 186 cm (dimensions Surface Hub 2S
85-inch. 44.5-inch x 77.1-inch x 3.4-inch (1130mm x 1959mm x 85.6mm)
pPerCM = 10.325 'pixel per cm
'how far away the loom starts - x(t) at t = 0 | if calculated as per physics doc, 350 (final
diam) * 80 (screen distance) / 6.5 (init diam)= 4307.69 cm
```

```
startDist = 1200 'cm
'ending distnace from the circle to the subject (not sure which formula applies)
endDist = -40 'cm
' the distance from the subject to the screen
screenDist = 60 'cm
' the initial speed when accelerating in cm perms
startSpeed = 0
'final diam = x(0) *6.5 (init diam)/screen distance
circleDiam = 130 'cm
trialNumber = 0
' using this data we write a function that gives us the size of the circle in pixels on the
' screen for a given distance of the circle to the subject
' you find this function in the user script (Alt-5), it is called "GetDiam()"

        ''''''''''''''''''''''''''''''''''''''''''''''''''''
        ' InLine - StimulusInit BEGIN <StimulusInit>
        ''''''''''''''''''''''''''''''''''''''''''''''''''''
Dim diameter As Double
Dim attentionStart As Long
Dim frameTime As Long 'time elasped
'Dim startRadius As Double using startDist inside GetDiam
Dim angle As Double
Dim stimulusStartDelay As Long
Dim distance As Double
Dim acceleration As Double
Dim endSpeed As Double
Dim duration As Integer
Dim rotationSpeed As Double
Dim pieNumber As Integer
Dim st As String

st = c.GetAttrib("LoomDuration")
st = Mid$ (st, 4, 4)
duration = CInt (st) 'duration of looming in millisec

Dim qo As String
qo = c.GetAttrib("RotationSpeed")
qo = Mid$ (qo,7, 6)
rotationSpeed = CDbl (qo)/1000 'angular speed in deg per millisec

Dim er As String
```

```
er = c.GetAttrib("ColoredPies")
pieNumber = CInt (er) 'Half the number of total pies


endSpeed = (startDist - endDist) * 2 / duration
acceleration = (endSpeed - startSpeed) / duration
trialNumber = trialNumber + 1


        ''''''''''''''''''''''''''''''''''''''''''''''''''''
        ' InLine - FixationRotation BEGIN <FixationRotation>
        ''''''''''''''''''''''''''''''''''''''''''''''''''''
diameter = GetDiam(startDist)
attentionStart = Clock.ReadMillisec
frametime = Clock.ReadMillisec - attentionStart
Do
        angle = frameTime * rotationSpeed * PI/180 'taken as degrees inside the pie
        'pi/180 multiplied to scale down the 5500 value - 5500*3.1415/180 ~ 95.99 | not
converting to radians
        Wheel diameter/2, pieNumber, angle
        Redraw
        frameTime = Clock.ReadMillisec - attentionStart
        'Debug.Print "angle" & angle
Loop Until frameTime >= attentionDuration


        ''''''''''''''''''''''''''''''''''''''''''''''''''''
        ' InLine - LoomingWheel BEGIN <LoomingWheel>
        ''''''''''''''''''''''''''''''''''''''''''''''''''''
stimulusStartDelay = TargetBegin.OnsetTime - attentionStart
frameTime = Clock.ReadMillisec - TargetBegin.OnsetTime
Debug.Print TargetBegin.OnsetTime
Do
        'Debug.Print "duration: " & (frameTime - lastFrameTime) ?? where is lastframetime??
        ' calculate the rotation, based on the start of the attention (could also simply be
Clock.ReadMillisec-attentionstart)
        angle = (frameTime + stimulusStartDelay) * rotationSpeed * PI/180 'taken as degrees
inside the pie
        'pi/180 multiplied to scale down the 5500 value - 5500*3.1415/180 ~ 95.99 degrees per
second | not converting to radians
        ' the virtual distance
        distance = startDist - startSpeed*frameTime - acceleration*frameTime^2/2

        ' the diameter of the circle
        diameter = GetDiam(distance)
        Wheel diameter/2, pieNumber, angle
```

```
        Redraw
        frameTime = Clock.ReadMillisec - TargetBegin.OnsetTime
Loop Until frameTime >= duration
Debug.Print Clock.ReadMillisec & "  " & c.GetAttrib("CellLabel")

        ''''''''''''''''''''''''''''''''''''''''''''''''''
        ' InLine - ClearScreen BEGIN <ClearScreen>
        ''''''''''''''''''''''''''''''''''''''''''''''''''
realCanvas.FillColor = backgroundColor
realCanvas.Clear
Debug.Print trialNumber

NUlab_UserBreak c, TrialList, True
```

1d *Participant consent form*

NTNU

Project Date: 05 Apr 2022
Project Reference: Audrey van der Meer

Faculty of Social Sciences and Education
Department of Psychology
Developmental Neuroscience Laboratory (Nu-Lab)

REQUEST FOR PARTICIPATION IN THE RESEARCH PROJECT

VISUAL MOTION & MOTOR CONTROL IN ADULTS

EEG-Study of the Brain

We want to find out how the adult brain processes visual motion as well as the relationship between motor control and visual motion. This is a pilot study to understand brain responses to ecologically rich stimuli in adults.

WHAT DOES THE PROJECT INVOLVE?

The study involves a single session at the Neuroscience Development Laboratory at NTNU Dragvoll (approx. 1.5 -2 hours). You will wear an electrode net that detects electrical brain activity, while watching animations and playing computer games on a large screen.

SAFETY

Your task is to look at moving things on the screen while wearing the electrode net. The examination is harmless and will not cause any discomfort. If participation in the project should give rise to suspicion of illness or injury, you can be referred to the correct health service.

Postal address
7491 Trondheim
Norway

Org.nr. 974 767 880
kontakt@ips.ntnu.no
http://www.ntnu.no/psykologi

Visiting address
Nu-lab
Bygg 12, nivå 2 (12-296)
NTNU Dragvoll

Telephone
+47 73 59 19 60

VOLUNTARY PARTICIPATION AND CONSENT

It is voluntary to participate in the project. We will contact you and if you wish to participate, you sign the declaration of consent on the last page and submit it upon meeting with us. You can withdraw your consent at any time and without giving any reason. If you withdraw from the project, you can demand that the collected data and information be deleted, unless the information has already been included in analyses or used in

scientific publications. If you later want to withdraw or have questions about the project, you can contact Audrey van der Meer, tel. 918 97 522, audrey.meer@ntnu.no.

DATA PRIVACY

The information registered about you should only be used as described for the purpose of the project. You have the right to access the information that is registered about you and the right to have any errors in the information that is registered corrected.

All information will be processed without name and birth number or other directly recognizable information. A code links you to your information through a list of names. Only the project manager and project coordinator have access to this list. It will not be possible to identify you when the results are published. If you have participated in this study before, we would like to compare past and present information.

INSURANCE

The Patient Injuries Act applies to your examination at NTNU Dragvoll.

FUNDING

The project is partly funded by NTNU and the equipment is funded by the Norwegian Research Council.

APPROVAL

The regional committee for medical and health research ethics has assessed the project and has given prior approval (Case number 2013/636).

You have the right to complain about the processing of your information to the Data Inspectorate.

CONTACT INFORMATION

If you have questions about the project, contact:

Project Staff:	Audrey van der Meer	audrey.meer@ntnu.no	tel: 918 97 522
Privacy representative at the institute:		Thomas Helgesen	thomas.helgesen@ntnu.no.

I AGREE TO PARTICIPATE IN THIS PROJECT AND ALLOW THE USE OF MY PERSONAL INFORMATION AS DESCRIBED

Place and Date

Participant's Signature

Participant's name in BLOCK letters

I CONFIRM TO HAVE PROVIDED THE PROJECT INFORMATION

Place and Date

Signature

Role in Project

Appendix 2: **Supplementary information for Results Section**

2a *Table with relevant participant details for obtaining results*

Age	**Case**	**Condition**	**Accepted Trials**	**Interpolated**	**Bad**
		4-0	22/16		
27	Ak	3-0	24/20	23	11
		2-0	19/17		
		0	23/18		
		4-0	29/20		
23	Av	3-0	29/26	8	10
		2-0	30/24		
		1-0	28/24		
		0	30/22		
		4-0	30/28		
26	I	3-0	26/25	5	14
		2-0	27/25		
		0	29/28		
		4-0	17/15		
23	M	3-0	16/9	12	20
		2-0	23/22		
		1-0	21/19		
		0	21/14		
		4-0	30/28		
27	O	3-0	30/29	1	0
		2-0	30/29		
		0	30/29		
		4-0	30/20		
25	R	3-0	30/19	21	31
		2-0	30/16		
		0	30/22		

27	Ab	4-0	30/29		
		3-0	30/30	3	7
		2-0	30/29		
		1-0	30/27		
		0	30/27		
		4-0	30/30		
22	Ti	3-0	30/30	11	15
		2-0	30/29		
		1-0	30/30		
		0	30/29		
		4-0	29/25		
27	Sh	3-0	29/25	4	20
		2-0	30/23		
		0	30/26		
		4-0	30/11		
31	St	3-0	30/14	0	12
		2-0	30/16		
		0	29/12		
		4-0	30/28		
23	T	3-0	30/24	1	2
		2-0	30/28		
		0	30/27		
		4-0	30/28		
24	V	3-0	30/26	6	6
		2-0	30/25		
		0	30/26		

2b *TSE Composites for 12 participants no-target condition*

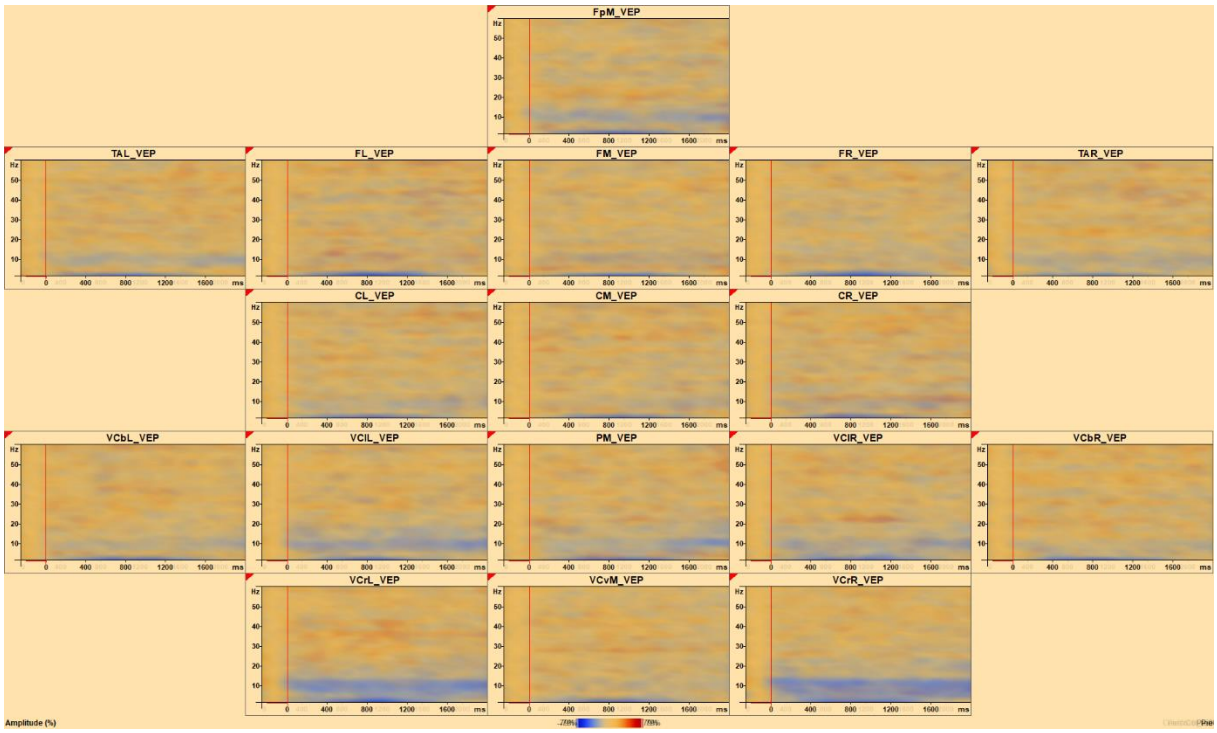

Pie0

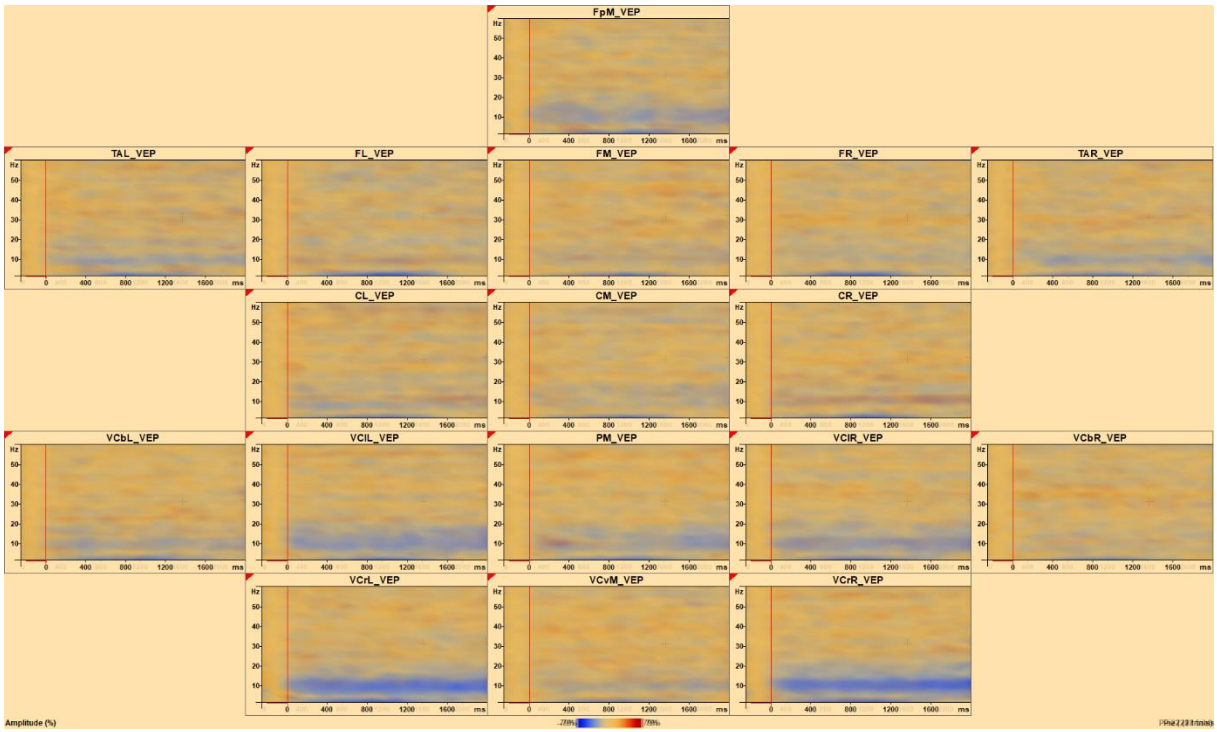

Pie2

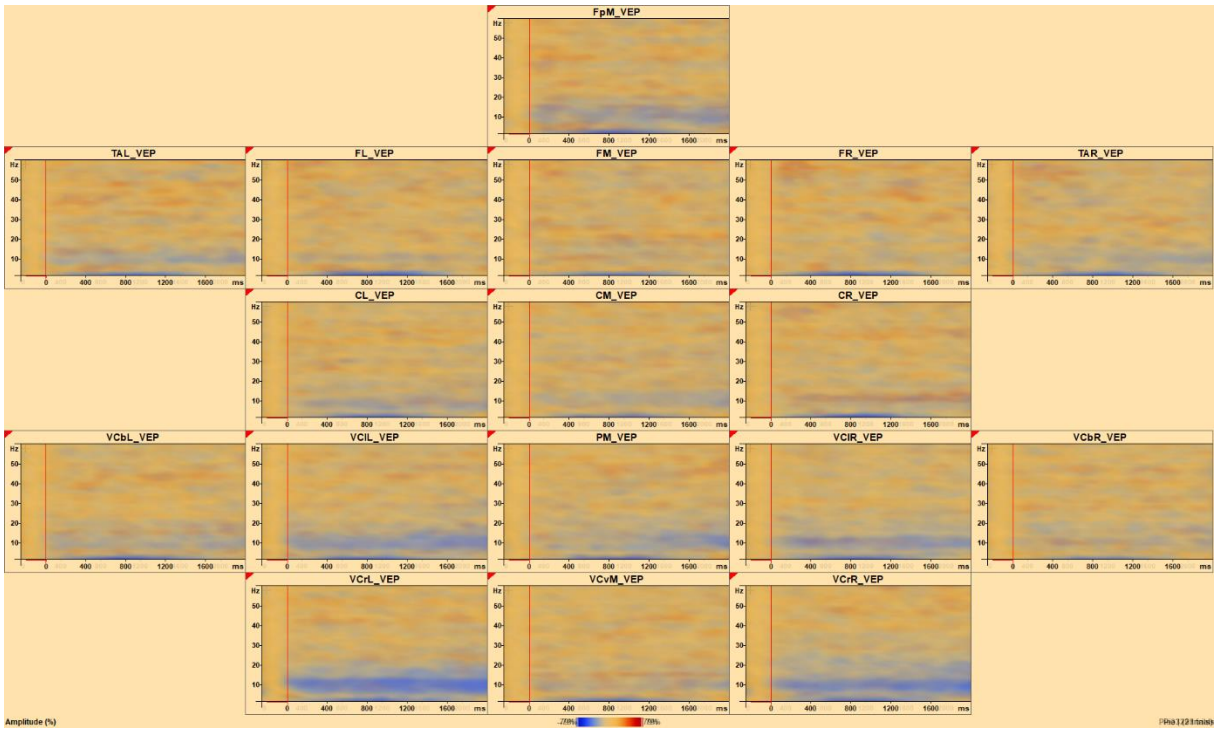
FpM_VEP
TAL_VEP
FL_VEP
FM_VEP
FR_VEP
TAR_VEP
CL_VEP
CM_VEP
CR_VEP
VCbL_VEP
VCIL_VEP
PM_VEP
VCIR_VEP
VCbR_VEP
VCrL_VEP
VCvM_VEP
VCrR_VEP
Amplitude (%)

Pie3

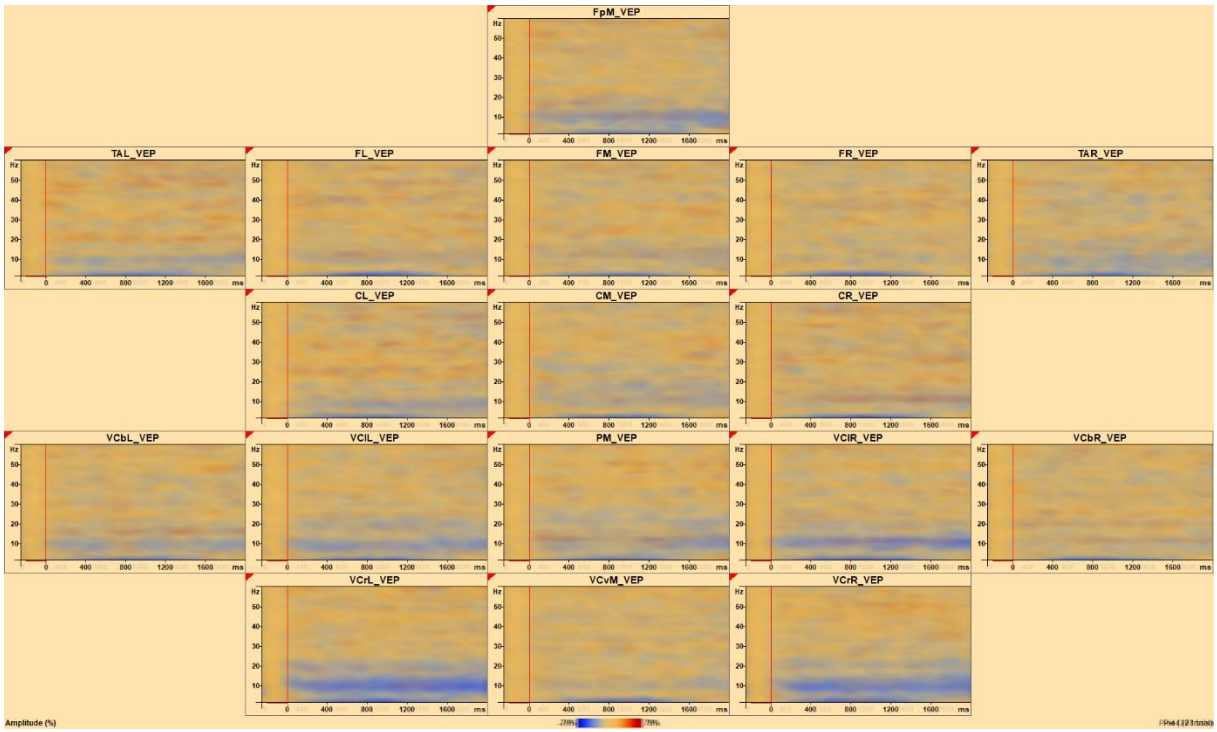
FpM_VEP
TAL_VEP
FL_VEP
FM_VEP
FR_VEP
TAR_VEP
CL_VEP
CM_VEP
CR_VEP
VCbL_VEP
VCIL_VEP
PM_VEP
VCIR_VEP
VCbR_VEP
VCrL_VEP
VCvM_VEP
VCrR_VEP
Amplitude (%)

Pie4

2c *TSE Composites for 12 participant target-vs-control condition*

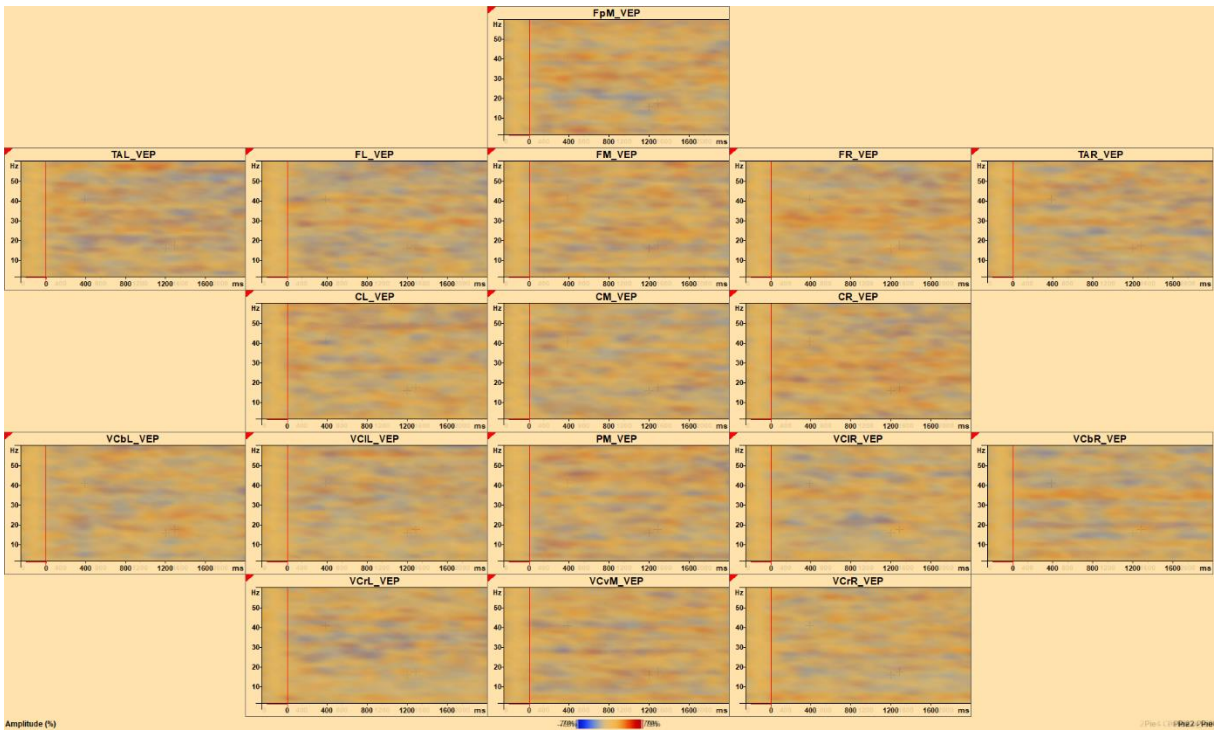

(a) Pie2-Pie0

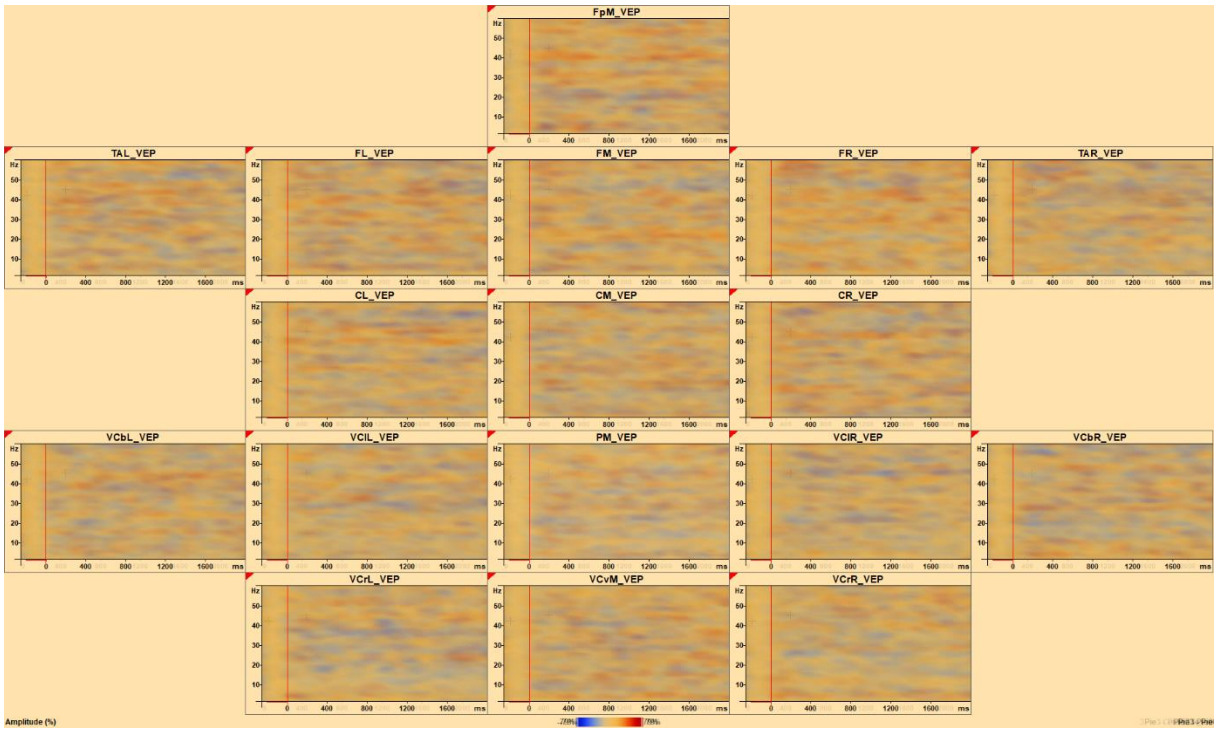

Pie3-Pie0

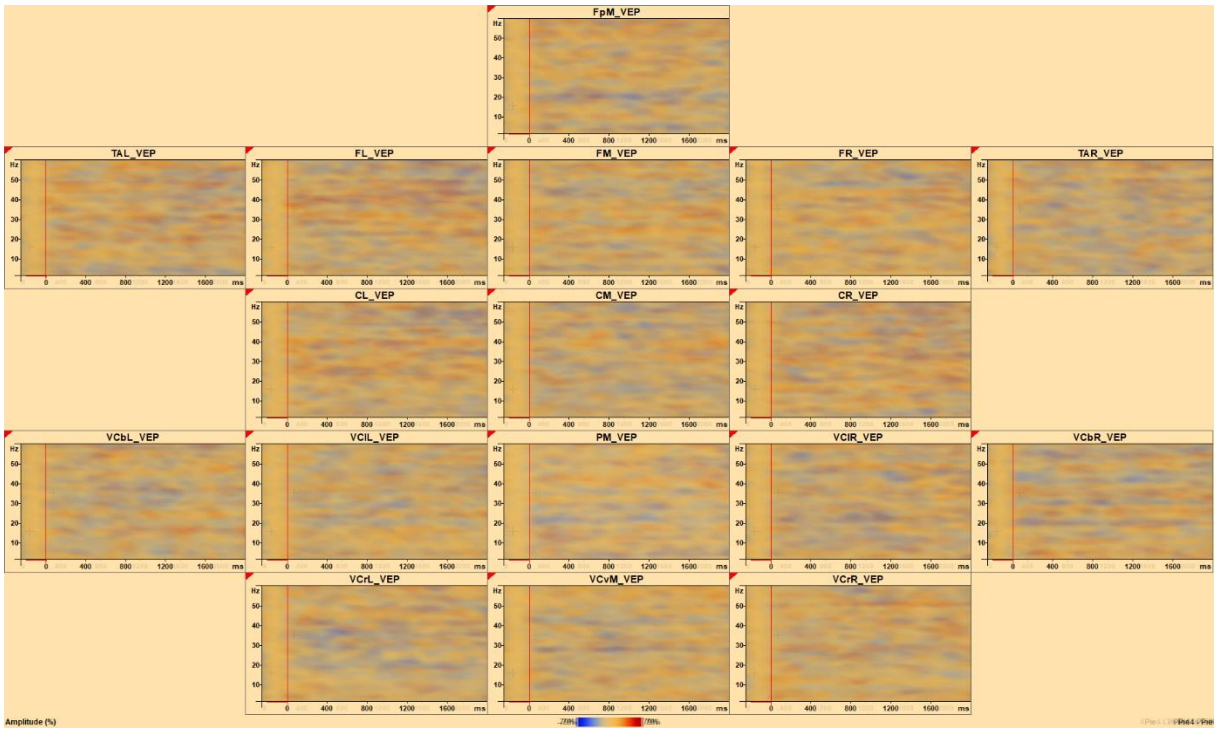

Pie4-Pie0

2d *Case O_b Pixel Plot for VCrL – resolution 5Hz 10ms*

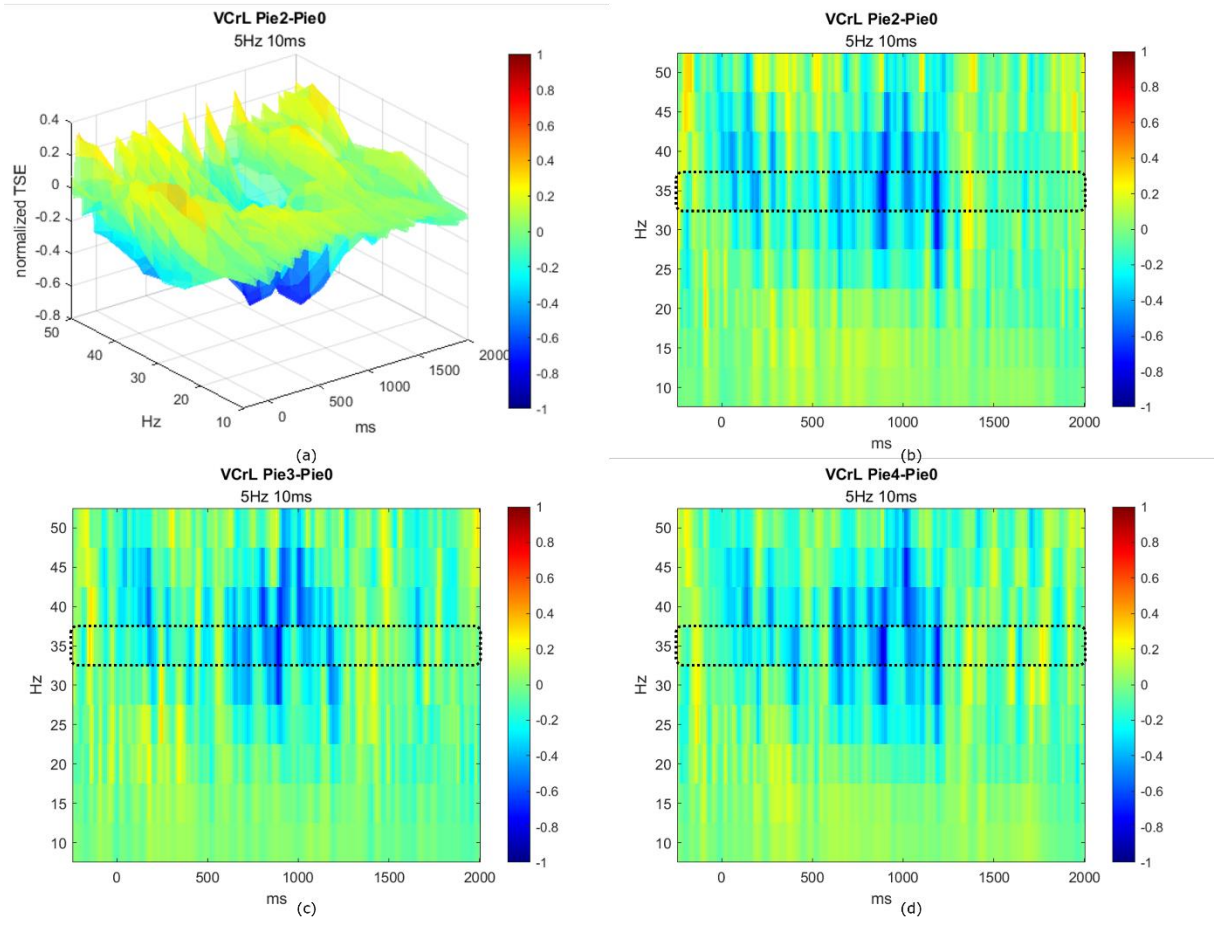

2e *Comparison of TSE bands and Frequency components of 5Hz 10ms with 2.5Hz 20ms resolution.*

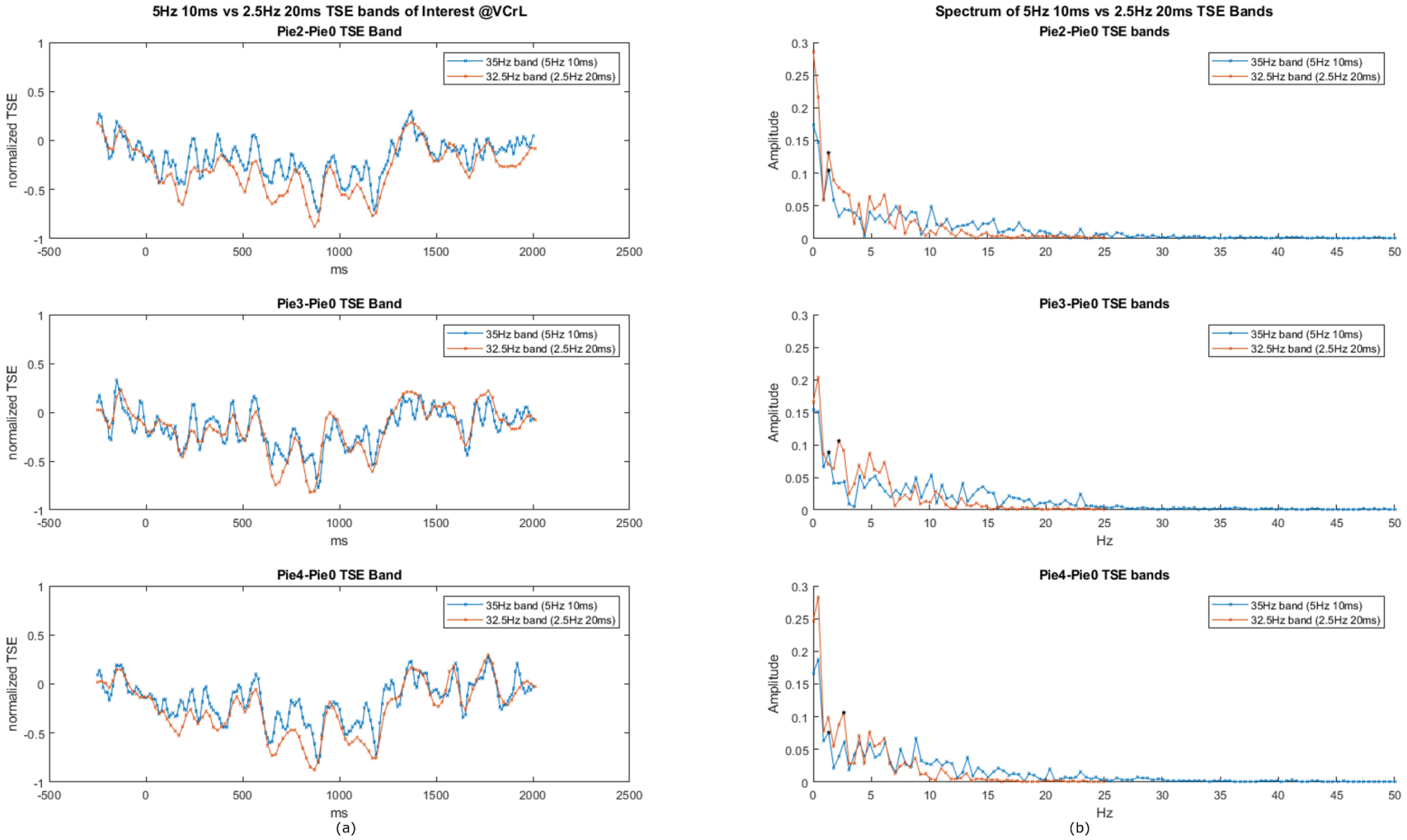

2e *Table showing the values obtained for Participant T which did not give a good linear fit*

Case	Condition	Tau rotation	Good Trials (total 30)	Source Channel	Frequency Band (Hz)	FFT Component	FFT Amplitude
T_a	Pie2	0.53316	28	VCbL	22.5	3.0701	0.1438
2.5Hz 20ms	Pie3	0.799753	24	VCbL	22.5	1.3157	0.1070
	Pie4	1.06633	28	VCbL	22.5	3.0701, 6.1403	0.1455, 0.0596
T_b	Pie2	0.53316	28	VCbL	25	3.0701	0.1621
2.5Hz 20ms	Pie3	0.799753	24	VCbL	25	0.4385	0.1056
	Pie4	1.06633	28	VCbL	25	3.0701, 5.7017	0.1529, 0.0944

2f *Pixel plot for Participant T @VCbL (showing highest ERD in Visual Cortex source channels)*

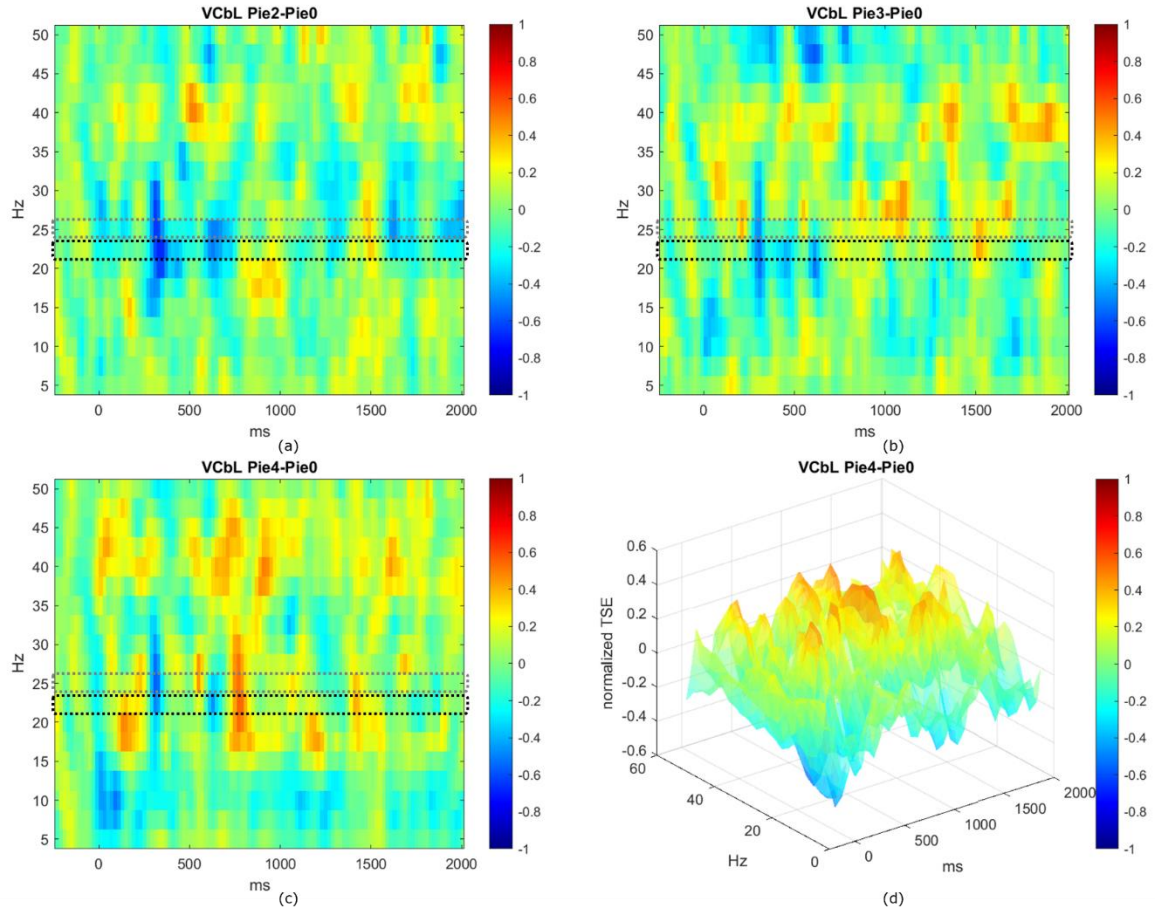

2g *Frequency bands of interest – 22.5 Hz and 25 Hz @ VCbL and their FFT magnitudes*

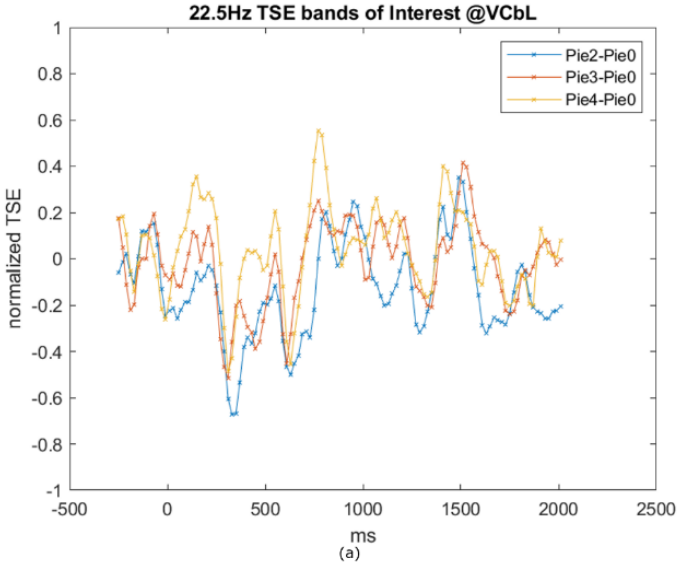

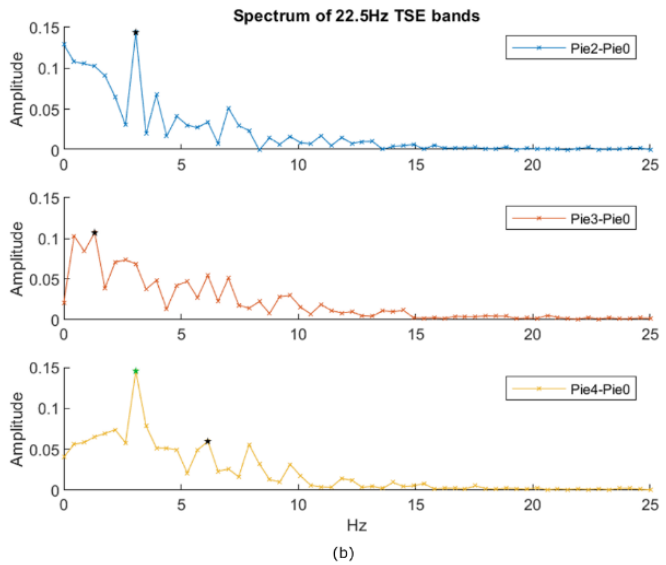

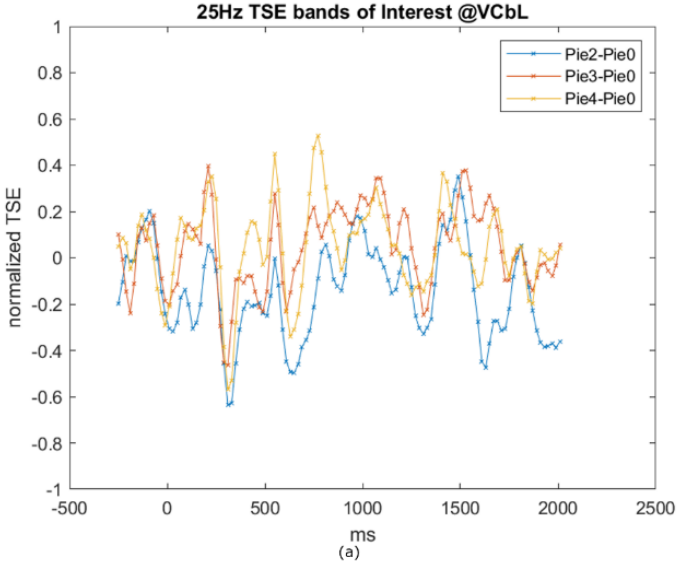

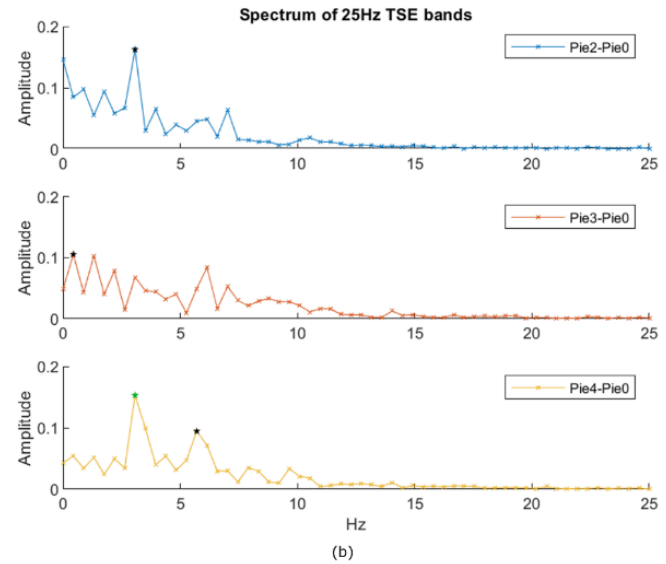

Appendix 3: Supplementary Information for Discussion section

3a *2d Fourier transform of the trajectory of diametrically opposite points gives a pattern of 2Pie.*